The retention of black holes in globular clusters

Wuxueman Liu

Lund Observatory
Lund University

2021-EXA185

Degree project of 60 higher education credits (for a degree of Master)
May 2021

Supervisors: Ross Church and Daohai Li

Lund Observatory
Box 43
SE-221 00 Lund
Sweden

Abstract

October 8, 2021

We simulate the velocities of formed Black Holes to determine the fraction of retained Black Holes in 152 Globular Clusters. The model we used for the escape velocity is from Plummer. The scenarios of the natal kick are Neutron-star like kicks and momentum conserving kicks. We also consider the binary fraction which affect the retention of Black Holes. A typical Globular Cluster retains 0 or 10^2 Black Hole with NS-like kicks or momentum conserving kicks respectively in the simulation which only consider Black Holes as single stars. If the binary fraction f_b is three quarters, a typical Globular Cluster retains $10^{2.5}$ Black Holes with two scenarios.

Popular summary

Wuxueman Liu

September 2021

The Black Hole are popular objects in astronomy, a lot of scientists want to study their formation and evolution. Most astronomers agree with that there is a super massive black hole in the center of our galaxy. Also, some previous observations show that at least some clusters have black holes. As we all known, a typical black hole is formed by a core-collapse supernova of a massive star. The core-collapse supernova is a explosion that blow out material surrounding the core, so the star always looses the majority of its mass and only leave one core. The mass of this massive stars has a upper limit, extremely massive stars will not become black hole but disappear during their evolution. Here comes a conclusion that the mass of a typical black hole is smaller than stellar black holes in some clusters or the super massive black hole in the center of our galaxy. This means, those massive black holes may be produced by the merger of some smaller black holes.

One possible pathway of formation of the surrounding material of super massive black holes is the merger of globular clusters that spiralled into the center. If we want to produced such super massive black holes, the globular cluster must have some black holes. The core-collapse supernova is a asymmetric explosion, the force from different directions are not the same. The black hole may get a natal kick from this explosion. Because of the natal kick, the velocity of black holes may be enough to escape from the host cluster. The magnitude of the black hole natal kick is very unclear, unlike neutron stars, which emit pulses of radio waves as they rotate, black holes can not be observed directly. In this project, I simulate two kinds of kick in 152 globular clusters(from Harris'

database). If the natal kicks of black holes are exactly the same as neutron stars, only a handful of black holes can be retained in the cluster. If the natal kicks of black holes are reduced by the mass relations of BH-NS, hundreds to thousands of black holes remain.

However, most of massive stars are in binary systems. The companion of the black holes in binaries also affects the retention of the black hole. The companion may slow down the black hole after the explosion. If the massive star interact with the companion before become a black hole, the merger and common-envelope evolution of binary will affect the velocity of the black hole. I simulate those globular clusters with three quarters of massive stars in binaries. Both kinds of kick could let a typical globular cluster retain hundreds of black holes.

In conclusion, a typical globular cluster can retain hundreds of black holes in this simulation. The case of the kick is the same as neutron stars should be ruled out if most massive stars are not in binaries.

The retention of black holes in globular clusters

Wuxueman Liu

supervisor:Ross Church

subspervisor:Daohai Li

April 2021

Contents

1 Introduction

In this project, I study the retention of Black Holes (BHs) in Globular Clusters (GCs). 'Retention' means the fraction of BHs that remain in the GC after the supernovae in which they form. From this study, I want to understand how the cluster properties like mass and metallicity affect the retention of BHs and measure the uncertainty of this prediction.

Some previous studies (Kormendy and Richstone, 1995) show that there is a super massive black hole (SMBH) in our galactic center. The formation pathway of SMBHs is still uncertain, one possible scenario being related to binaries. The BH can exchange with one star of a binary in a gravitational interaction, this process is more likely in stellar areas with high density of stars (like the GC). One observation is the radio and X-ray emission from X-ray binary 47 Tuc X9 in the GC 47 Tuc (NGC104) shows that a stellar-mass BH is accreting mass from the companion carbon-oxygen WD (Church et al., 2017). This system may be formed by the collision of a stellar-mass black hole with a giant star. When one X-ray binary with a main-sequence star (also can be a red giant star or a neutron star) and a BH collide with a single BH, the main-sequence star

will be ejected and leave one BH-BH binary. Two BHs in the BH-BH binary then will merge and produce a more massive black hole which can be the 'seed' of the SMBH in the Galactic Center (Askar et al., 2021). This is because one possible pathway of formation of the surrounding Nuclear Stellar Cluster (NSC) of SMBH is the merger of GCs that spiralled into the Galactic Center (Antonini et al., 2012, Renaud et al., 2017). In this case, BHs are brought by the clusters which hold enough BHs to form more massive BHs(intermediate BH (IMBH) with mass over $100M_{\odot}$), therefore studying the retention of BHs in clusters could help us to understand our galaxy.

GCs have several features. Most GCs are older than open clusters (OCs), they have the age around 12.8 Gyr (Forbes and Bridges, 2010). Hundreds of BHs formed during the first 10 Myr after formation (Larson, 1984), making it impossible to directly observe the evolution of massive stars in GCs. The GCs are massive, so they can live longer than OCs and the gravitational potential of stars are deeper than other stellar clusters (Sanchez-Lavega, 2011). These deeper potential makes the BHs more likely to be retained. Also, GCs are used as laboratory to study stellar physics (stellar evolution and dynamics) because the larger density of stars in GCs lead to more frequent stellar interaction (Binney et al., 2009).

In this work, the reasons I choose GCs are: (a) The larger density of stars lead to frequent stellar interactions, there are more interacting (X-ray) binaries which are formed by retained BHs in these clusters (Larson, 1984, Kundu et al., 2002, Arca Sedda et al., 2018) ; (b) Because the initial mass function is universal (Kroupa, 2001), massive clusters like GCs contain more massive stars, BHs progenitors, than others. (c) The deeper potential makes the BHs more likely to be retained. (d) Only GCs have enough BHs and binaries to form IMBH. (e) Denser clusters like GCs do not get tidal disruption like OCs during the in-falling to the Galactic Center.

BHs are formed after the supernovae that occur at the end of the life of massive stars. The BH or Neutron star (NS) is expected to receive a natal kick when it forms. This natal kick comes from the asymmetric explosion of

supernovae (Helfand and Huang, 1987), giving a kick velocity to the BH or NS. The evidence of BH natal kick is that the BHs are found in large distance from galactic plane today Repetto et al. (2012). The magnitude of BHs natal kicks is very unclear, unlike NSs, which emit pulses of radio waves as they rotate, BHs cannot be observed directly, so the BH kick velocity should be inferred indirectly. As the formation of NS and BH are similar, we can get the BH kick velocity using the relationship between natal kicks of NSs. Three scenarios are discussed in the astronomical literature. The first one is that the kick velocity of the BH is expected to be reduced by the mass ratio of the NS and BH in many pictures (Repetto et al., 2012) because they receive the same momentum. The second one is that the black hole in short-period low mass X-ray binary systems could receive either no natal kick or high natal kick in the formation (Repetto and Nelemans, 2015). The other simulation suggest BHs received similar natal kicks as NSs in the formation can suit the observed data (Repetto et al., 2017). The detail will be discussed in section.3. In this work, I consider the NS-like kick, reduced kick and zero-velocity kick both for single BHs and BHs in binaries under three different metallicities. The metallicity of GC affect the initial-final mass relation of star, then the final mass of BH may affect the kick velocity.

Another important parameter for calculating the retention fraction of BHs in GCs is the variation of escape velocity of BH from the cluster as a function of the BH's birth position. In this work, the model I use for the mass distribution of GC is Plummer's model (Plummer, 1911), which I fit to the observed properties of the GCs.

The retention fraction of single BHs can be simply calculated by a Monte-Carlo simulation of escape velocities and kick velocities. For each BH in the simulation, if the escape velocity is larger than the kick velocity then the BH is retained. These results are not sufficient, however, if GCs contain binary systems. Most of the massive stars which form BH are in binaries (Sana et al., 2012) and the companion of the BH progenitor then affects the velocity of BH after the supernova.

The companion of the BH in a binaries affects the retention of the BH

both by giving it an orbital velocity and by exerting gravitational force. The BH has an orbital velocity around the companion before the supernova, which depends on the distance between two stars and the masses of stars. When the supernovae happens, the kick velocity given by the natal kick and the orbital velocity combine to determine the final velocity of the formed BH. After the supernova, two stars will either remain bound or unbound. The retention of the bound binary can be describe by the relationship between the total velocity of the binary centre of mass and the escape velocity of this system. The unbound binary is not a single system but one star and one single BH, the retention of this BH depends on the relationship between the final velocity, the escape velocity of BH itself and the gravitational force from the previous companion.

In this paper, I will describe the project with 3 sections. In the section of GCs (sec.2), I will introduce the catalogue of GCs, calculate the total masses of GCs at birth and derive the function of escape velocities of BHs with the enclosed mass. Section 3 and 4 are about the BHs. In the Sec.3, I will discuss the value of BH kick velocity and calculate the numbers of retained BHs in GCs with the assumption that all the BHs progenitors are not in binaries. In the sec.4, I introduce the binary system, calculate the effect of natal kicks in binaries and discuss the retention of BHs in GCs with several assumptions of the fraction of binaries BHs in GCs.

2 Globular clusters

BHs receive a natal kick when they form, so they may be able to escape from GCs at birth. To investigate their retention we need to obtain the escape velocity at each position of our model globular clusters. The model I use is Plummer (1911) and the clusters' parameters are from Harris (1996) [1], including R_{sun} for the distance from the Sun, X, Y, Z for the location with $(0, 0, 0)$ for

[1]The paper is published in 1996 but the catalogue I use in the project is 2010 edition. The catalogue include 157 GCs but only 147 of them with the all data we want(the position, [Fe/H], integral magnitude, radius, etc.). We used 152 GCs in this project. 5 GCs do not have [Fe/H], so I used [Fe/H]=-5 for them.

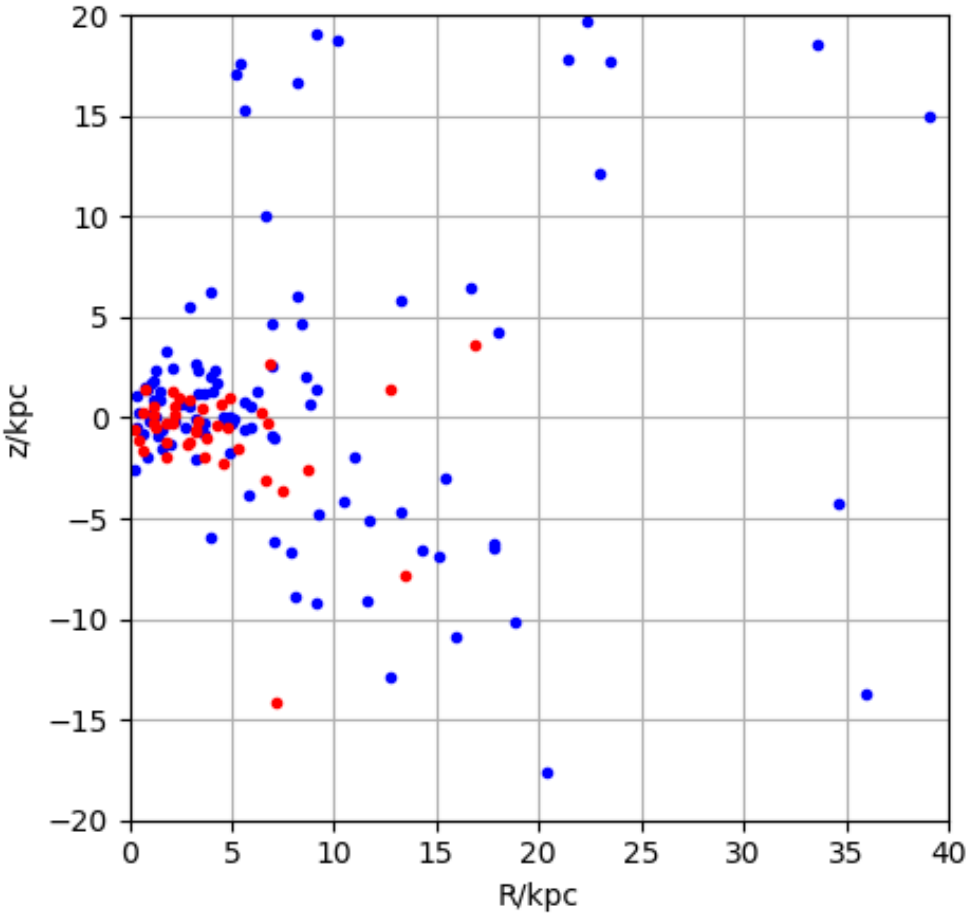

Figure 1: The figure of all GCs in our galaxy. The R,z positions are measured from the galactic center. The blue points are for the clusters with [Fe/H] lower than -1, and the red points are for clusters with [Fe/H] higher than -1.

galactic center, $[Fe/H]$ for metallicity, the integrated magnitude $M_{v,t}$ and half-light radius r_h in arcmin. The unit of R_{sun} and X, Y, Z is kpc.

2.1 Location

For the location of clusters, I plot Fig.1, where galactocentric cylindrical radius,

$$R = \sqrt{X^2 + Y^2} \tag{1}$$

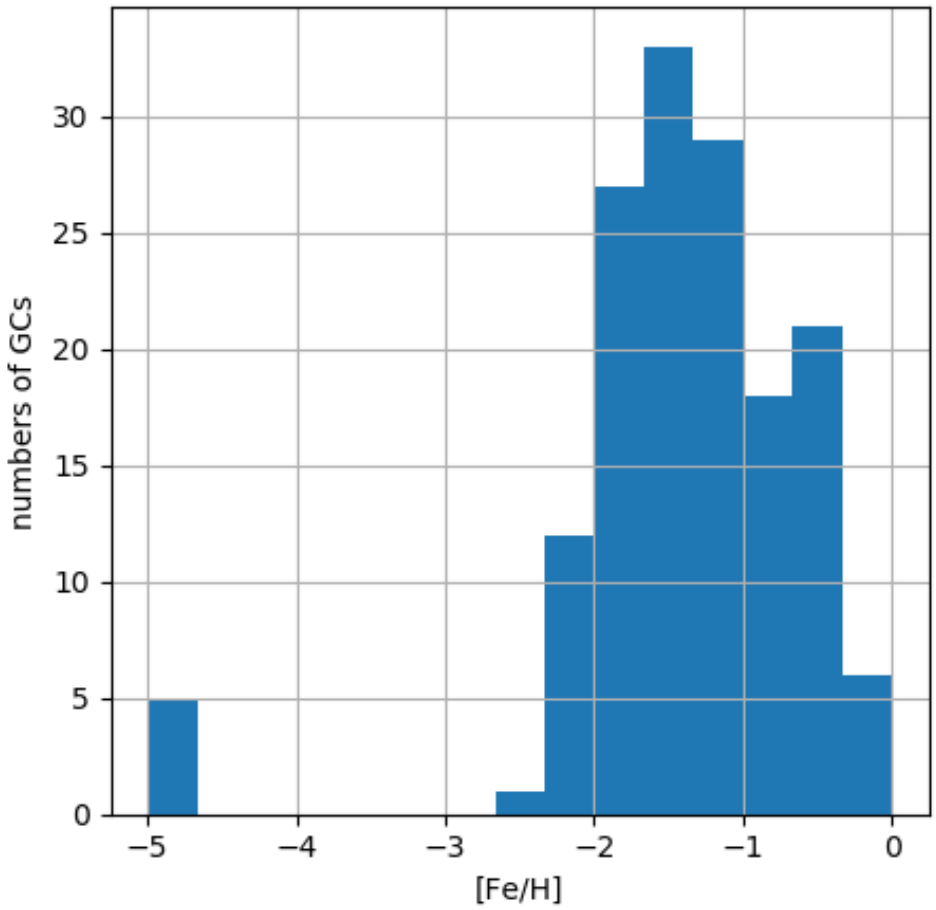

Figure 2: The histogram of GCs metalicities. Most of GCs have metalicities around -1.3, 5 GCs do not have [Fe/H], so I used [Fe/H]=-5 for them.

In the figure, the blue points are for the clusters with [Fe/H] lower than -1, and the red points are for clusters with [Fe/H] higher than -1. From the figure, we can divide these clusters into two groups. The 'disc-like' group, which are close to the galactic center in R are only a few kpc from the $z = 0$ disc. Almost all of the clusters with higher metallicity (red points) are in the 'disc-like' group. The 'halo-like' group have larger straight-line distances from the galactic center. Most clusters in this group have lower metallicity(blue points in Fig.1).

Mackey and Gilmore (2004) try to understand the origin of GCs observed in the galactic halo. They used high-quality photometry to analyze the morphology, structural and metallicities of external clusters and compare with other clusters. They found that all the young halo clusters and 15–17 percent of the old halo clusters are of external origin. This means the halo-like GCs may have not formed in Milky Way.

Renaud et al. (2017) want to figure out the formation and evolution of clusters. The reason for the colour and metallicities of GCs. They set the simulation with a flat-cold-dark-matter cosmology model of a Milky Way mass galaxy using the adaptive mesh refinement (AMR) code RAMSES (Teyssier, 2002) and considered the high-redshift and tidal field in the simulation of cluster formation. They get the result that the origin of low-metalicity clusters are external low-mass galaxies. The major of high-metalicity clusters are formed in Milky Way. This explain why most of halo-like clusters are low-metalicity.

The properties of 'disc-like' clusters is important for this project. BHs retained in 'disc-like' clusters are more likely to contribute to the central SMBH of the milky way because most stars in the NSC around SMBH have [Fe/H] higher than -0.5 (Thorsbro et al., 2020).

2.2 Mass

We do not have the clusters' mass in the catalogue, so we need to calculate it with the integrated absolute magnitude $M_{v,t}$ (t for total) and mass to light ratio. From the integrated absolute magnitude $M_{v,t}$, we can get the total luminosity

of the cluster as

$$\frac{L_t}{L_\odot} = 100^{\frac{M_{v,\odot}-M_{v,t}}{5}} \tag{2}$$

Where $M_{v,\odot} = +4.83$ is the absolute solar magnitude and $L_\odot = 3.828 \times 10^{26} W$ is the solar luminosity (NASA, 2010).

In this project, the mass to light ratio of all clusters I use is 2 (Binney et al., 2009). This is because the overwhelming majority of stars are less massive and less luminous than the Sun (mass-to-light ratio is greater than 1), and usually these stars contribute most of the mass of a system without accounting for very much light. So the total mass today of GC is

$$M = 2\frac{L_t}{L_\odot} M_\odot = 2 \times 100^{\frac{M_{v,\odot}-M_{v,t}}{5}} M_\odot \tag{3}$$

where M the total mass of cluster and $M_\odot$ the solar mass.

To investigate the retention of black holes, we cannot use these masses directly. As the clusters are evolving over time, the total mass of these clusters we have here are not the initial masses when the clusters formed. To estimate the initial mass, we can use the initial mass function of stars from Kroupa (2001).

The initial mass function,

$$\frac{dN}{dm} = km^{-\alpha} \tag{4}$$

From Kroupa(2001), $\alpha = 2.3$ for stars over 0.5 solar mass, $\alpha = 1.8$ for stars under 0.5 solar mass.

The function should be continuous at $0.5M_\odot$,

$$k'(0.5M_\odot)^{-1.8} = k(0.5M_\odot)^{-2.3} \tag{5}$$

$$k' = k(0.5M_\odot)^{-0.5} \tag{6}$$

The initial mass function under 0.5 solar mass is,

$$\frac{dN}{dm} = k(0.5M_\odot)^{-0.5} m^{-1.8} \tag{7}$$

The initial mass,

$$M(t=0) = \int_{m_{min}}^{m_{max}} \frac{dN}{dm} m dm = \int_{m_{min}}^{m_{max}} k m^{-\alpha} m dm \tag{8}$$

The m_{min} and m_{max} are $0.08 M_\odot$ and $100 M_\odot$ (Kroupa, 2001).

Assuming the number of stars in each cluster do not change from the beginning and the age of cluster is 14 Gyrs. From this age, stars have initial mass over $m_{today} = 0.8 M_\odot$ are white dwarf now. From the mass distribution of WD in De Gennaro et al. (2008), the average white dwarf mass is $0.55 M_\odot$.

The mass today,

$$M(t = 14Gyr) = \int_{m_{min}}^{m_{today}} k m^{-\alpha} m dm + M_{WD} \int_{m_{today}}^{10 M_\odot} k m^{-\alpha} dm \tag{9}$$

So we have,

$$M(t = 14Gyr) = \int_{0.08 M_\odot}^{0.5 M_\odot} k (0.5 M_\odot)^{-0.5} m^{-1.8} m dm \tag{10}$$

$$+ \int_{0.5 M_\odot}^{0.8 M_\odot} k m^{-2.3} m dm \tag{11}$$

$$+ 0.55 M_\odot \int_{0.8 M_\odot}^{10 M_\odot} k m^{-2.3} dm \tag{12}$$

$$M(t = 14Gyr) = 1.88892 k M_\odot^{-0.3} + 0.539699 k M_\odot^{-0.3} + 0.544257 k M_\odot^{-0.3} \tag{13}$$

$$= 2.972876 k M_\odot^{-0.3} \tag{14}$$

$$k = \frac{M(t = 14Gyr)}{2.972876 M_\odot^{-0.3}} \tag{15}$$

The initial mass,

$$M(t=0) = \int_{0.08 M_\odot}^{0.5 M_\odot} k (0.5 M_\odot)^{-0.5} m^{-1.8} m dm + \int_{0.5 M_\odot}^{100 M_\odot} k m^{-2.3} m dm \tag{16}$$

$$= 4.32211 k M_\odot^{-0.3} \tag{17}$$

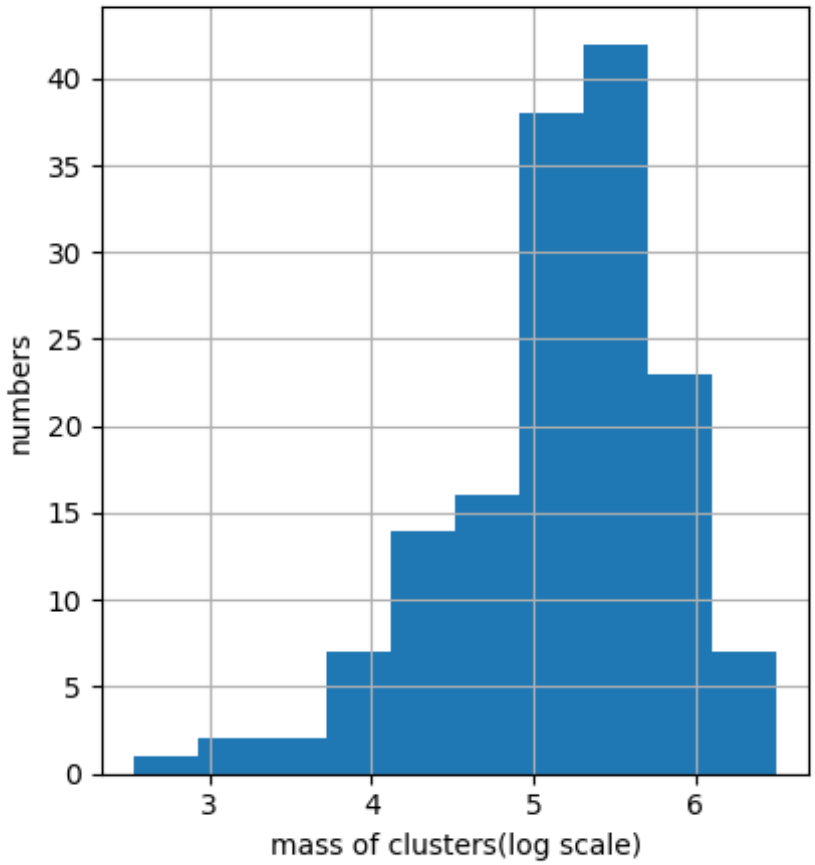

Figure 3: The histogram of GCs' initial mass. The x-axis is the log-scale of mass in solar mass. The y-axis is the numbers of clusters (152 in total).

$$M(t=0) = 4.32211 M_{\odot}^{-0.3} \frac{M(t=14Gyr)}{2.972876 k M_{\odot}^{-0.3}} = 1.453848 M(t=14Gyr) \quad (18)$$

The Fig.3 shows the distribution of GCs' mass at birth. Most clusters have a mass between 10^5 to 10^6 solar masses. The largest mass is about $10^{6.5}$ solar mass and the smallest mass is about $10^{2.5}$ solar mass.

2.3 Plummer's model

The model I use to describe the mass distribution of GCs for this project is Plummer's model (Plummer, 1911), including the mass with radius r (projected

radius d), the specific potential and the half-mass radius. It is is a density law that was first used by Plummer (1911) to fit observations of globular clusters. This model has simplest and useful definition of enclosed mass, potential and escape velocity.

In this model, the specific potential (potential per unit mass) is defined as

$$\phi(r) = -\frac{GM}{a}\left(1 + \frac{r^2}{a^2}\right)^{-1/2} \tag{19}$$

where a is the length scale parameter and r is the position of the star (radius from the cluster center).

The length scale parameter a sets the radial scale of the cluster model. It sets the spatial distribution of mass and hence the central escape velocity. To get the a from Harris' catalogue (Harris, 1996) , another equation from Plummer's model we need is the mass with projected radius,

$$M(d) = M\left(1 + \frac{a^2}{d^2}\right)^{-1} \tag{20}$$

where d is the projected distance from center of cluster to the star. As we have half-light radius r_h in arcmin and R_{sun}, The projected half-light radius d_h is

$$d_h = R_{sun} sin(r_h) \tag{21}$$

Assuming the mass to light ratio of one cluster is a constant, the half-light radius is also the half-mass radius. So we have

$$\frac{M}{2} = M(d_h) = M\left(1 + \frac{a^2}{d_h^2}\right)^{-1} \tag{22}$$

from this we have the length scale parameter,

$$a = d_h = R_{sun} sin(r_h) \tag{23}$$

The Fig.4 shows the distribution of a. The most of clusters have the length

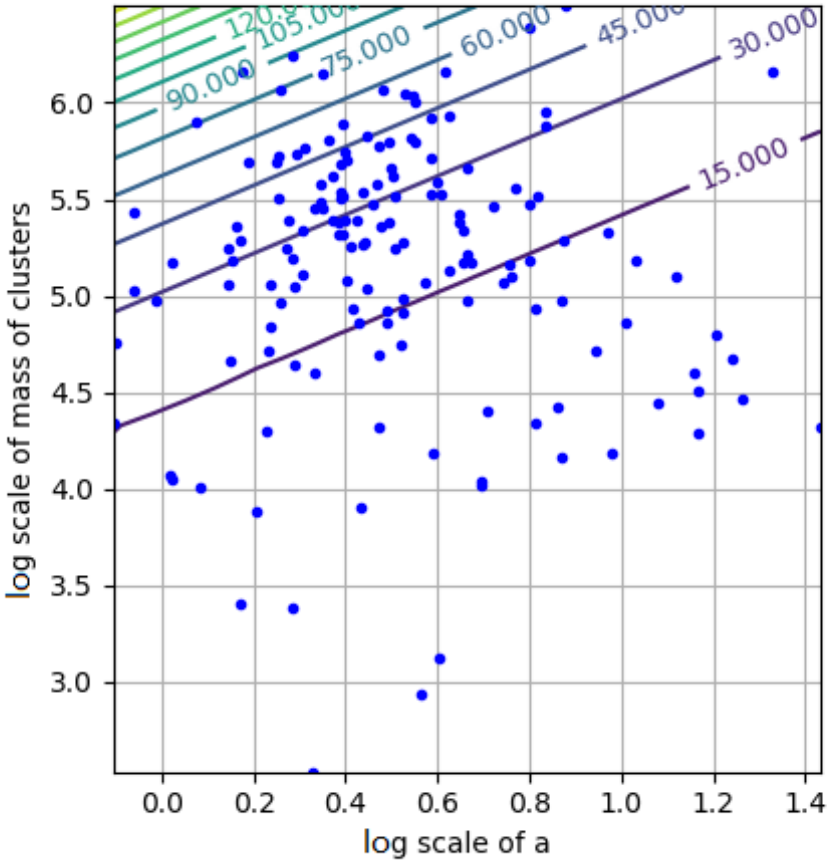

Figure 4: The scatter figure of length parameter a of plummer's model and clusters' mass. The x-axis is the log scale of a. The y-axis is the log scale of masses of clusters. The contour lines are central escape speed in km/s.

scale parameter a of few parsec and the total mass around 10^5 to 10^6 solar mass. The extended clusters with $a < 5pc$ have lower mass than others. The range of a is one parameter of the range of central escape velocities, which will be discussed in sec 2.5.

2.4 Escape velocity

The Escape velocity is a important part for studying the retention of black holes. For one star, we have the energy

$$\text{potential energy} + \frac{1}{2}mv^2 = \text{total energy} \tag{24}$$

for escape velocity,

$$\text{potential energy} + \frac{1}{2}mv_{esc}^2 = 0 \tag{25}$$

The potential Φ we have in Plummer's model is a specific potential (potential per unit mass), so

$$v_{esc} = \sqrt{-2\Phi} = \sqrt{\frac{2GM}{a}\left(1 + \frac{r^2}{a^2}\right)^{-1/2}} \tag{26}$$

2.5 Enclosed mass and central escape velocity

From Plummer's model (Plummer, 1911), we have the mass with position

$$m(r) = M\left(1 + \frac{a^2}{r^2}\right)^{-3/2} \tag{27}$$

where $m(r)$ is the enclosed mass of the cluster and M for total mass of the cluster.

We can rewrite the escape velocity in the radius of r like

$$v_{esc} = \left(\frac{2GM}{a}\right)^{1/2}\left(1 + \frac{r^2}{a^2}\right)^{-1/4} \tag{28}$$

From eq.27 and eq.28, we can get

$$v_{esc} = \left(\frac{2GM}{a}\right)^{1/2} \left(1 + \frac{1}{\left(\frac{M}{m(r)}\right)^{2/3} - 1}\right)^{-1/4} \tag{29}$$

Also we have the central escape velocity where $r = 0$

$$v_{esc,c} = \left(\frac{2GM}{a}\right)^{1/2} \tag{30}$$

So we have

$$v_{esc} = v_{esc,c} \left(1 + \frac{1}{\left(\frac{m(r)}{M}\right)^{-2/3} - 1}\right)^{-1/4} \tag{31}$$

The Fig.5.a shows $v_{esc}/v_{esc,c}$ as a function of enclosed mass fraction $m(r)/M$. This figure should be same for all clusters. The Fig.5.b is the histogram of $v_{esc,c}$ of all globular clusters.

3 Black holes

3.1 Black hole kicks

The Black hole may get a natal kick when it formed because the force is not isotropic. This natal kick gives a kick velocity v_{kick}. I use the distribution of kick velocities from the paper by Hobbs et al. (2005). The distribution of v_{kick} is a Maxwellian distribution with $\sigma = 265km/s$, (Fig.6). This distribution is for NSs. The relationship between $v_{kick,NS}$ and $v_{kick,BH}$ is still uncertain. BHs and NSs experience the asymmetric explosion caused by the ejection of material of their progenitors at birth. If a BH and a NS experience the same asymmetric explosion, they will receive the same momentum but $v_{kick,BH}$ is smaller than $v_{kick,NS}$ because the mass of the BH is larger. In this case,the $v_{kick,BH}$ should be reduced by the ratio of BH mass to NS mass. As the asymmetric explosion depends on the mass-loss of the BHs progenitors, if the BH do not eject material in the explosion, it will not get a kick velocity.

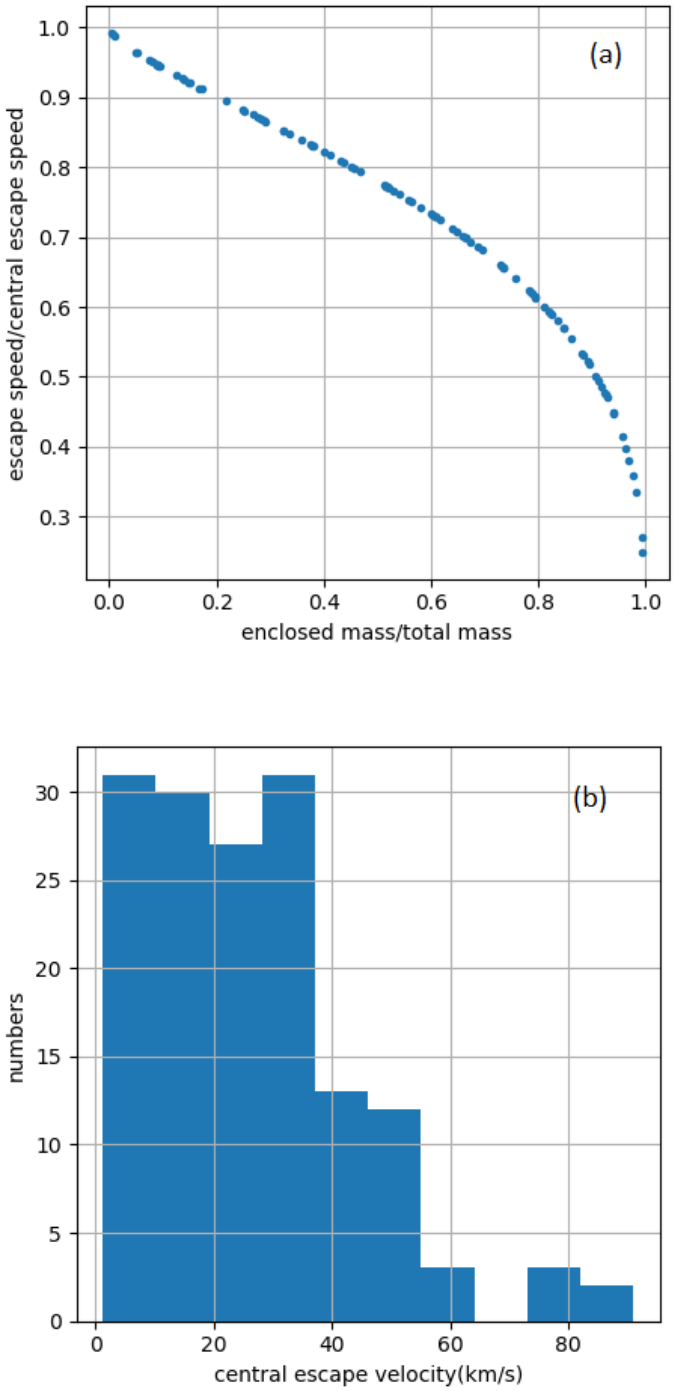

Figure 5: (a) The figure of $v_{esc}/v_{esc,c}$ and enclosed mass fraction $m(r)/M$. The x-axis is enclosed mass fraction, which means the ratio of mass inside the surface of radius to the total mass. This relationship is universal in Plummer's model. (b) The histogram of central escape velocity $v_{esc,c}$ for all gobular clusters. The x-axis is the $v_{esc,c}$ in km/s.

Repetto et al. (2012) tried to explain the distribution of low mass X-ray binaries with black holes in our galaxy by the natal kicks received by black holes. They simulated those binaries with several types of kicks from supernova mass-loss and natal kicks. The types of natal kicks that they simulated are zero km/s kick, NS kicks distribution from the Hansen and Phinney (1997), the bimodal distribution of Arzoumanian et al. (2002), reduced kicks (multiply by M_{NS}/M_{BH}) of Hansen and Phinney (1997) and reduced kicks of Arzoumanian et al. (2002). They found that the black holes should receive natal kicks because they are found at large vertical distances from the galactic plane today. The natal kicks of black holes have a similar distribution to the neutron stars, but it is expected to be reduced by the mass ratio of the neutron star and black hole in many other pictures. From this, we can estimate the distribution of black hole natal kicks directly from a natal kick distribution of neutron stars in our work.

Repetto and Nelemans (2015) consider the uncertainty of the magnitude of natal kick in the formation of black holes. They find seven short-period low mass X-ray binary systems with orbiting period shorter than one day. They traced the evolution of these binaries backward to the formation and added other kinematic information for binaries. The result is that the black hole in these binaries could receive either no natal kick or high natal kick in the formation process. We should consider the zero kick velocity case in our work.

Repetto et al. (2017) wanted to figure out which model of black hole and neutron star natal kick could explain the galactic distribution of X-ray binaries. They simulate the whole evolution of neutron star and black hole X-ray binaries in several models. They compared the simulation to the observed data of galactic distribution and used KS-test for comparison. They found that the neutron stars will have a larger scale-height above the galactic plane than black holes as observed data if they received similar natal kick in the formation process. This paper also tell us that we can use the natal kick distribution of neutron stars for black holes in our work.

Mandel (2016) wanted to find the highest estimated black hole natal kick velocity from observations of black hole low-mass X-ray binaries. They consider a binary found in position a of the galactic plane and remove to the position b. The natal kick velocity can be estimated from the difference in the Galactic potential between position a and b. They showed that the observation do not require large black hole natal kick at the order of 400 km/s, the maximum require of natal kick velocity is 80 km/s. These results are compatible either with a full NS-like kick or a reduced kick.

These articles present three scenario of BH natal kick:(a) The momentum conserving kick: The BH receive the same momentum as NS, so the $v_{kick,BH}$ should be reduced by the ratio of BH mass to NS mass.(b) The NS kick: The distribution of $v_{kick,BH}$ is exactly the same as this of $v_{kick,NS}$.(c) The zero kick velocity: The BH do not receive natal kick because it did not lose mass during the supernova. I will consider these three conditions in my simulation.

3.2 Numbers of BHs retained in GCs

3.2.1 Numbers of formed BHs in GCs

To calculate the numbers of BHs retained in these GCs, we need the numbers of formed BHs in GCs at first.

The initial mass function,

$$\frac{dN}{dm} = km^{-\alpha} \tag{32}$$

From Kroupa (2001), $\alpha = 2.3$ for stars over 0.5 solar mass, $\alpha = 1.8$ for stars under 0.5 solar mass.

The function should be continuous at $0.5M_{\odot}$,

$$k'(0.5M_{\odot})^{-1.8} = k(0.5M_{\odot})^{-2.3} \tag{33}$$

$$k' = k(0.5M_{\odot})^{-0.5} \tag{34}$$

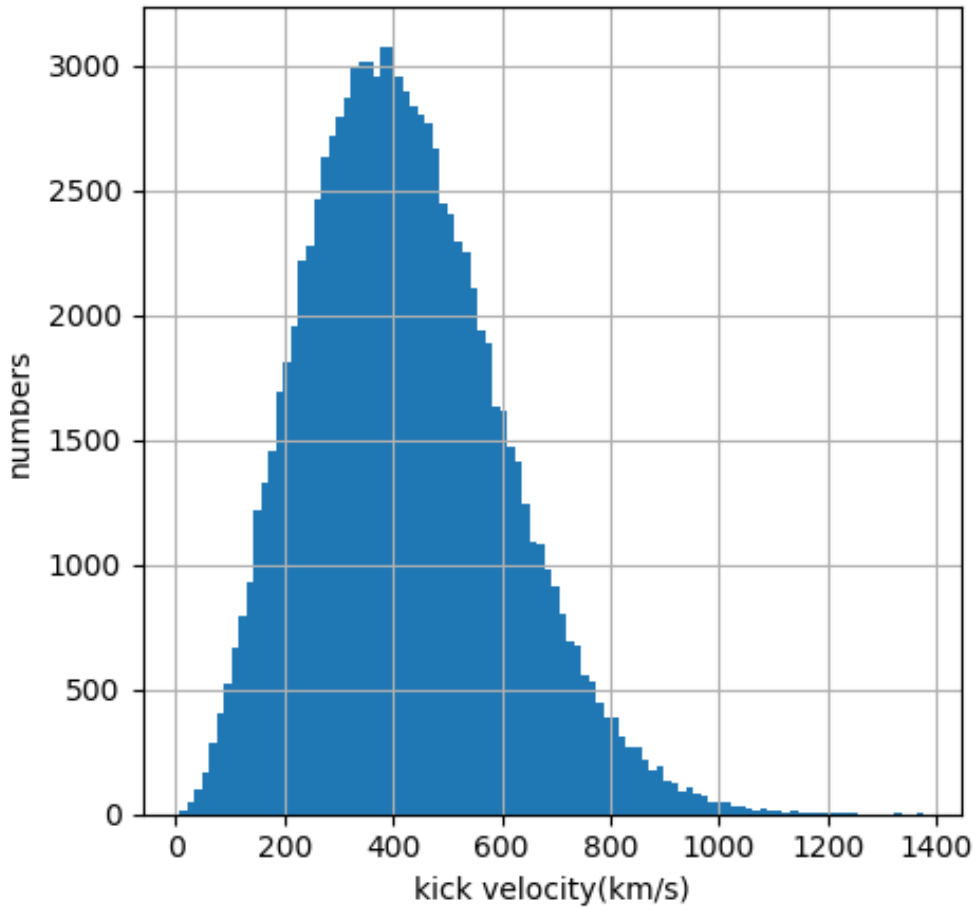

Figure 6: The Maxwellian distribution of v_{kick} with $\delta = 265km/s$ from Hobbs et al. (2005)

The initial mass function under 0.5 solar mass is,

$$\frac{dN}{dm} = k(0.5M_{\odot})^{-0.5}m^{-1.8} \tag{35}$$

From the initial mass function, we can get the fraction of massive stars which can be the BHs progenitors. The lower limit I set for BHs progenitors is 20 $M_{\odot}$ (Davies and Beasor, 2020), the star under this mass will produce a White Dwarf or a Neutron Star. The upper limit I set is 70 $M_{\odot}$ (Woosley, 2017), the star over this mass undergo an instability during Oxygen burning which makes the temperature of the core high enough to create free electron positron pair and blows the star apart by a pair-instability supernova (Fraley, 1968). So, the star with initial mass larger than 70 $M_{\odot}$ will not become a BH. As I said in the introduction, massive BHs in our galaxy may be produced by the merger of smaller BHs. Using the same of Eq.8 for the total number and masses of stars, the relationship between the number of BHs (N_{BH}) and the total number of stars (N) is

$$\frac{N_{BH}}{N} = \frac{\int_{20M_{\odot}}^{70M_{\odot}} km^{-2.3}dm}{\int_{0.08M_{\odot}}^{0.5M_{\odot}} k(0.5M_{\odot})^{-0.5}m^{-1.8}dm + \int_{0.5M_{\odot}}^{100M_{\odot}} km^{-2.3}dm} \tag{36}$$

$$= \frac{0.0125853}{12.148} \tag{37}$$

$$= 0.001036 \tag{38}$$

Also the total number of stars,

$$N = \int_{0.08M_{\odot}}^{0.5M_{\odot}} k(0.5M_{\odot})^{-0.5}m^{-1.8}dm + \int_{0.5M_{\odot}}^{100M_{\odot}} km^{-2.3}dm = 12.148kM_{\odot}^{-1.3} \tag{39}$$

As we already calculate the k and the total initial mass of cluster in Eq.15 and Eq.17,

$$k = \frac{M}{4.32211M_{\odot}^{-0.3}} \tag{40}$$

$$N = 12.148kM_{\odot}^{-1.3} \times \frac{M}{4.32211M_{\odot}^{-0.3}} = 2.81066MM_{\odot}^{-1} \tag{41}$$

So the number of formed BHs is

$$N_{BH} = 0.001036N = 0.001036 \times 2.81066MM_{\odot}^{-1} = 0.002912MM_{\odot}^{-1} \tag{42}$$

The histogram of formed BHs in GCs is the 'a' part of Fig.7.a, most of GCs can form 10^3 BHs.

3.2.2 Scenario of NS-like kick

To calculate the retention fraction of BHs in one GC, I generate random kick velocities from the Maxwellian distribution of Harris (1996) and random positions for 10^5 BHs and their progenitors. For each BH, I compare the kick velocity v_{kick} with escape velocity v_{esc} which is calculated from the position of BH and the central escape speed of GC using Eq.27. If the black hole is retained after the supernova, it should have v_{kick} smaller than v_{esc}. The retention fraction of this GC can be describe like $N_{retained,BHs}/N_{formed,BHs}$.

3.2.3 Scenario of momentum conserving kick

For reduced kick, we should consider the final mass of the BH after the supernova because the momentum of the BH and the NS kick are the same. To calculate this, we use the Initial-Final Mass Relation which was calculated using the stellar evolution routines of Hurley (2000) and the core mass - remnant mass relation of Belczynski et al. (2002). The IFMR is the relationship between the mass of the BH progenitor and the BH under given metallicity. For example, one $20M_{\odot}$ star will become a $2.332M_{\odot}$ BH after supernova in a solar metallicity ([Fe/H]=0) cluster. Because we do not have data of IFMR with every metallicities, I used solar metallicity([Fe/H]=0), [Fe/H]=-2 and [Fe/H]=-1.3 in this project. The [Fe/H]=-1.3 is a common metallicity for GCs, the Fig.2 shows this. We assume that the metallicities of GCs today (Harris, 1996) is equal to the metallicities of GCs at birth. Fig.8, Fig.9 and Fig.10 show the tendency of

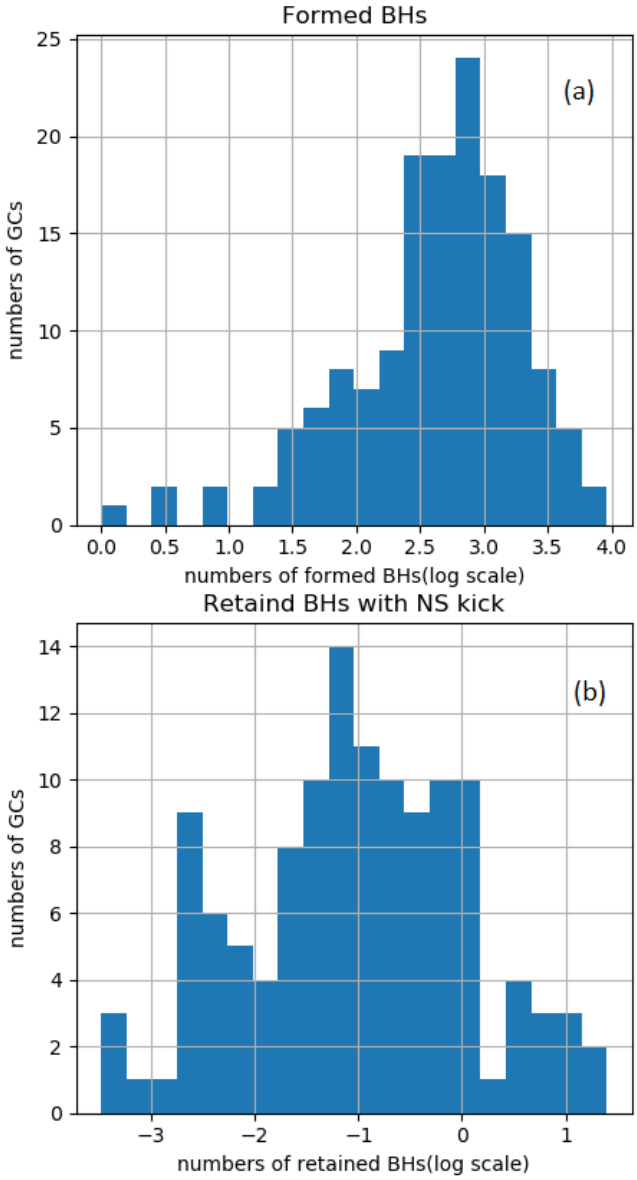

Figure 7: (a) The histogram of formed BHs in GCs, most of GCs can form 10^3 BHs. (b) The histogram of retained BHs in GCs with NS-like kick, most of GCs can not retain BHs.

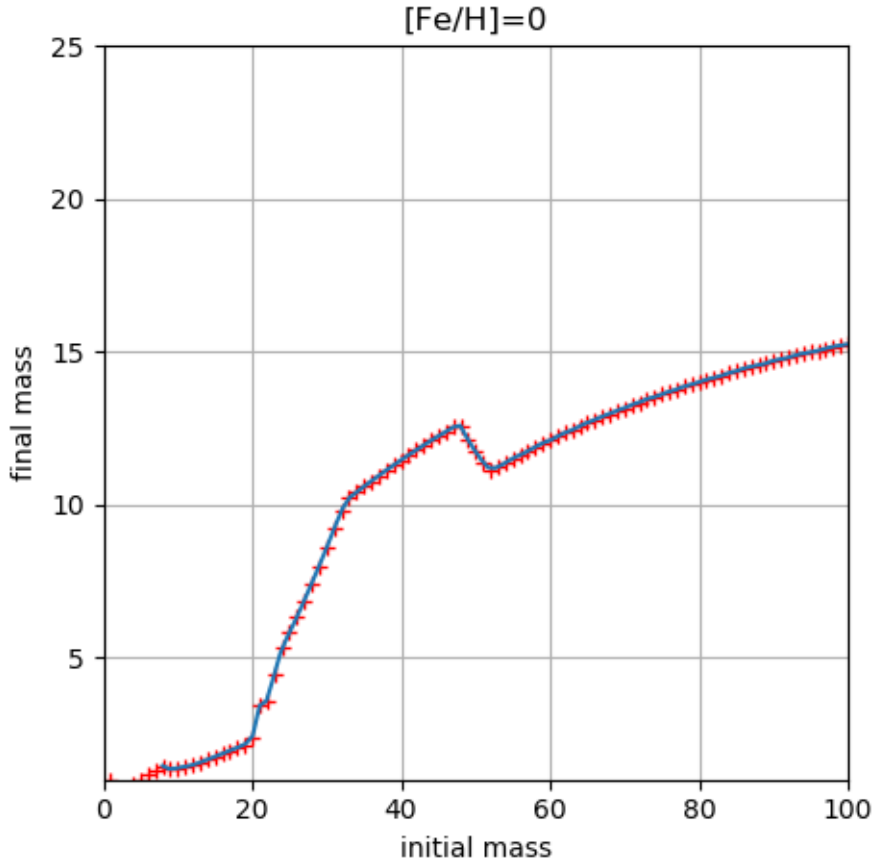

Figure 8: The figure of IFMR data and fitted line with solar metallicity ([Fe/H]=0). The method I use is linear interpolation. The x-axis is the initial mass of the BH progenitor and the y-axis is the final mass of the BH in solar mass units.

IFMR and the fitted line I used for following calculations. For a star has the same initial mass, the final mass of it is smaller in higher [Fe/H] than lower [Fe/H]. This is because the cluster with higher metallicity has stronger winds.

For each GC, I generate 10^5 stars with initial mass between $20M_\odot$ and $70M_\odot$ from IMF (Kroupa, 2001) and calculate the final mass of BHs from the initial mass and IFMR. The reduced kick velocity is

$$v_{kick,reduced} = v_{kick,NS}\frac{1.4M_\odot}{M_{BH}} \tag{43}$$

where $1.4M_\odot$ is the typical mass of NS (Seeds and Backman, 2009).

I compare the $v_{kick,reduced}$ with v_{esc} of each BH using the same procedure as

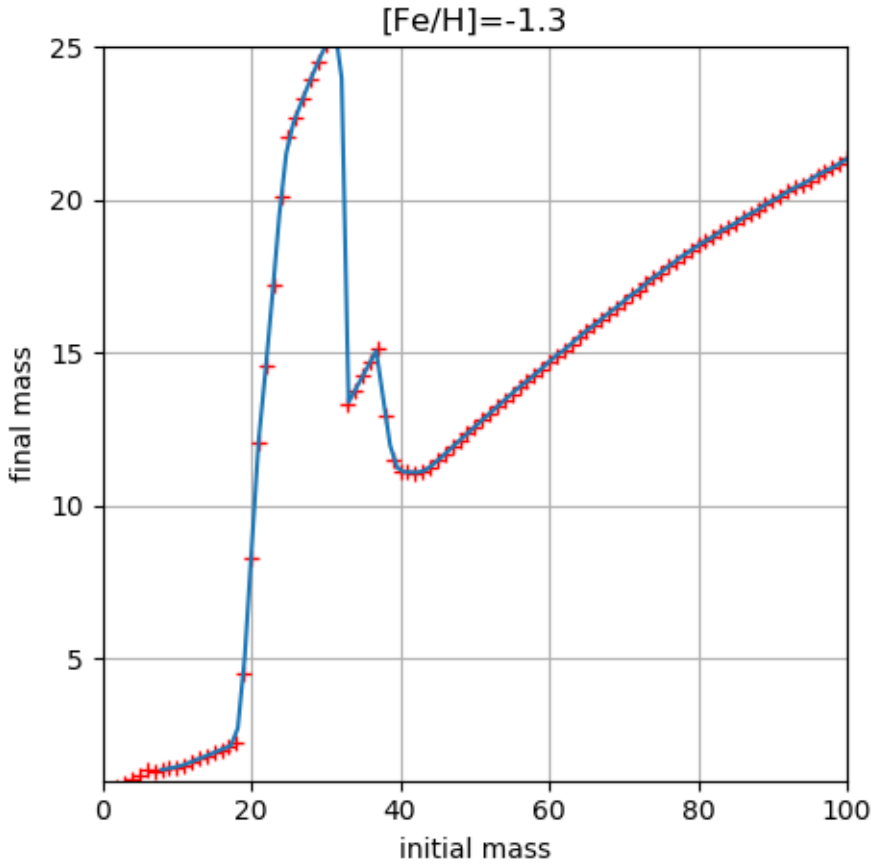

Figure 9: The figure of IFMR data and fitted line with $[Fe/H] = -1.3$. The method I use is linear interpolation. The x-axis is the initial mass of the BH progenitor and the y-axis is the final mass of the BH in solar mass units. The strange peak between 20 and 40 solar mass is the maximum mass of a Neutron star because the IFMRs of the NS and the BH are different.

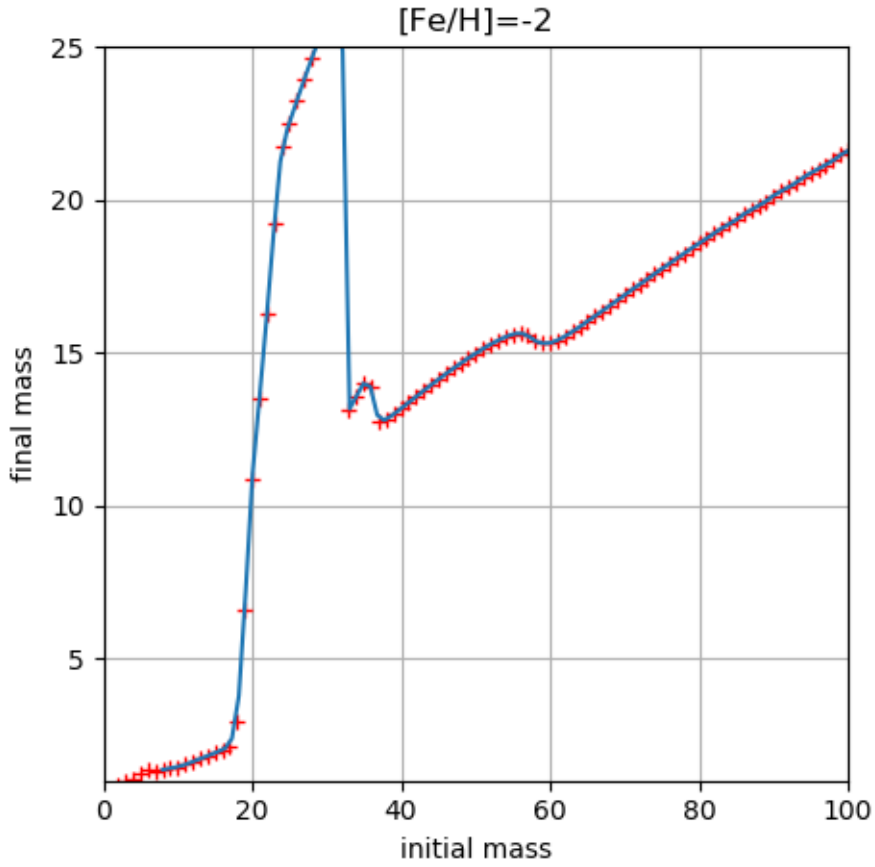

Figure 10: The figure of IFMR data and fitted line with $[Fe/H] = -2$. The method I use is linear interpolation. The x-axis is the initial mass of the BH progenitor and the y-axis is the final mass of the BH in solar mass units. The strange peak between 20 and 40 solar mass is the maximum mass of a Neutron star because the IFMRs of the NS and the BH are different.

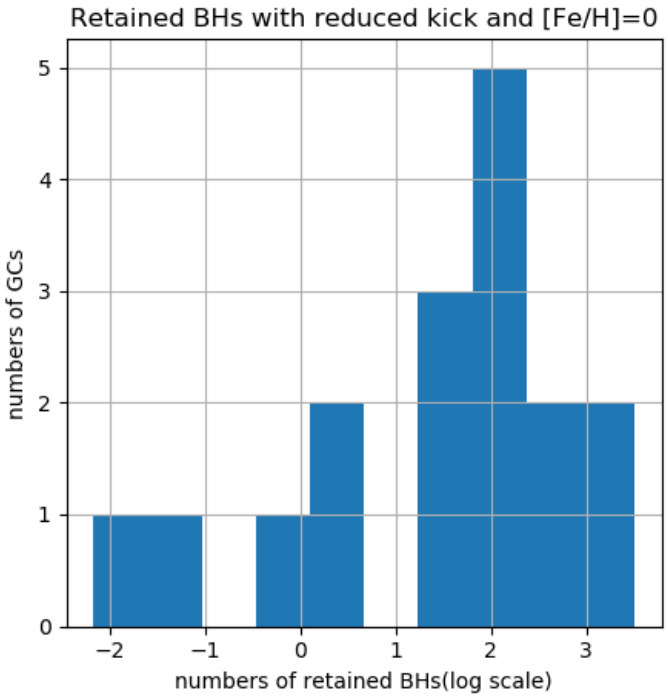

Figure 11: The histogram of retained BHs in GCs with reduced kick under [Fe/H]=0. Most of GCs retain about 10^2 BHs. The x-axis are the log scale of BHs numbers and y-axis are GCs numbers.

for NS-like kick and get the retention fraction of each GC. The Fig.14.a shows the distribution of NS-kick, reduced kick with [Fe/H] equal 0 and -1.3. Most of BHs can have kick velocity around 30 km/s or 50 km/s with [Fe/H]=0 or -1.3 respectively.

Fig.11, Fig.12 and Fig.13 show the histogram of retained BHs in GCs with reduced kick under [Fe/H]=0,-1.3 and -2. Most of GCs retain about 10^2 BHs.

3.2.4 NGC104

For globular cluster NGC 104:

1. The number of formed BHs is 4243.

2. The number of retained BHs with NS-like kick is $4243 \times 1.27 \times 10^{-3} = 5(5.389)$.

3. The number of retained BHs with reduced kick([Fe/H]=-1.3) is 4243 $\times$

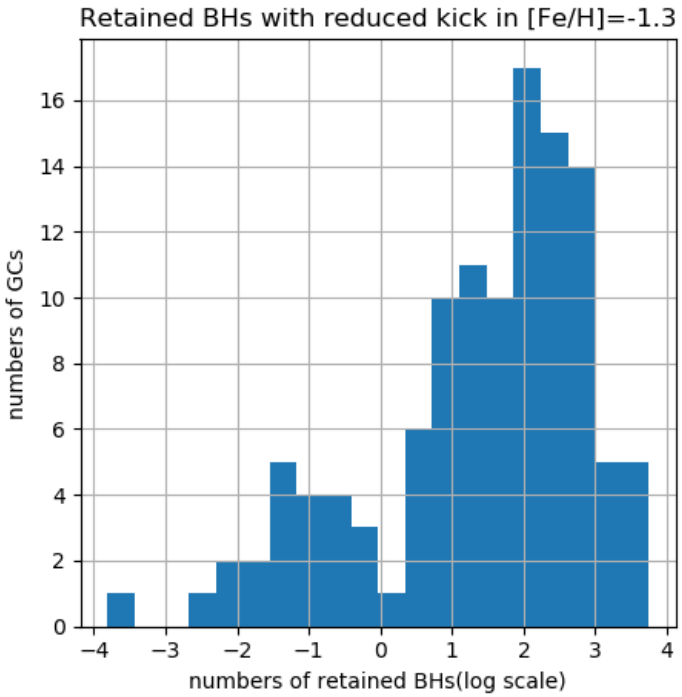

Figure 12: The histogram of retained BHs in GCs with reduced kick under [Fe/H]=-1.3. Most of GCs retain about 10^2 BHs. The x-axis are the log scale of BHs numbers and y-axis are GCs numbers.

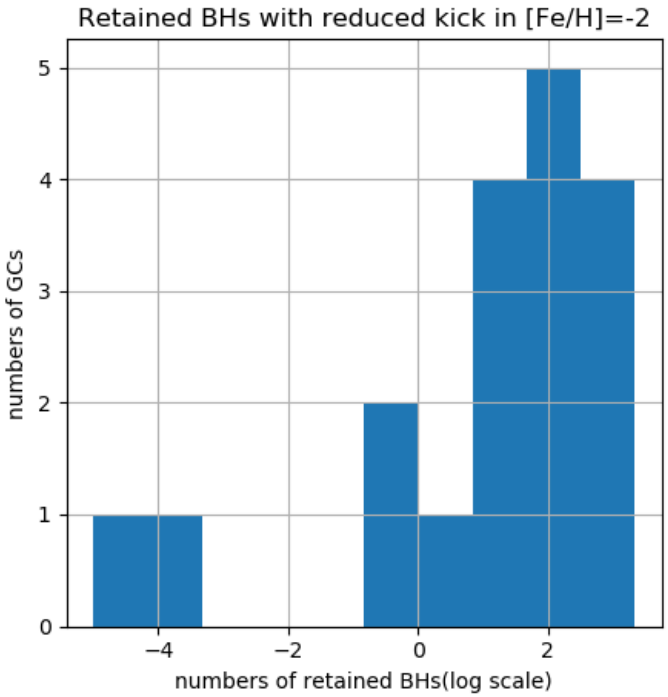

Figure 13: The histogram of retained BHs in GCs with reduced kick under [Fe/H]=-2. Most of GCs retain about 10^2 BHs. The x-axis are the log scale of BHs numbers and y-axis are GCs numbers.

$0.552 = 2342(2342.88)$.

The Fig.14.b shows the BHs in NGC104 with reduced kick(with [Fe/H]=-1.3) velocity, there are 10^5 BHs but not the number of formed BHs, the central escape speed is the data of NGC104. Massive BHs are easier to be retained in NGC104.

3.3 Results

Under the assumption that all BHs progenitors in GCs are not in binary system, the results:

1. For the NS-like kick, parameters are total mass and 'a' scale of GCs. The distribution of kick velocities is the Fig.6. The Fig.7.b shows the retained BHs in GCs with NS-like kick. There are only a few BHs are retained in a typical GCs if BHs receive NS-like kicks.

2. For the reduced kick, another parameter is the metallicities of GCs which are relative to the magnitude of kick reduction. The Fig.11, Fig.12 and Fig.13 shows the retained BHs in GCs with [Fe/H] equal 0, -1.3 and -2 respectively. Compare to the NS-like kick, most of GCs retained more BHs with reduced kick. As we only have the data of IFMR with [Fe/H] equal 0 ,-2 and -1.3, I suggest that most of GCs could use [Fe/H]=-1.3. For GCs with [Fe/H] under -0.5 and over -2, we use [Fe/H]=0 and -2 respectively. Most of GCs have [Fe/H] around -1.3, gives a broad range of numbers of retained BHs. But from the Fig.15, results mostly depending on the masses of the clusters.

4 Binary systems

Another important part of this investigation into the retention of black holes are binary systems. Most of the black hole progenitors are found in binary systems. Black holes that form in binary system are more likely to be retained

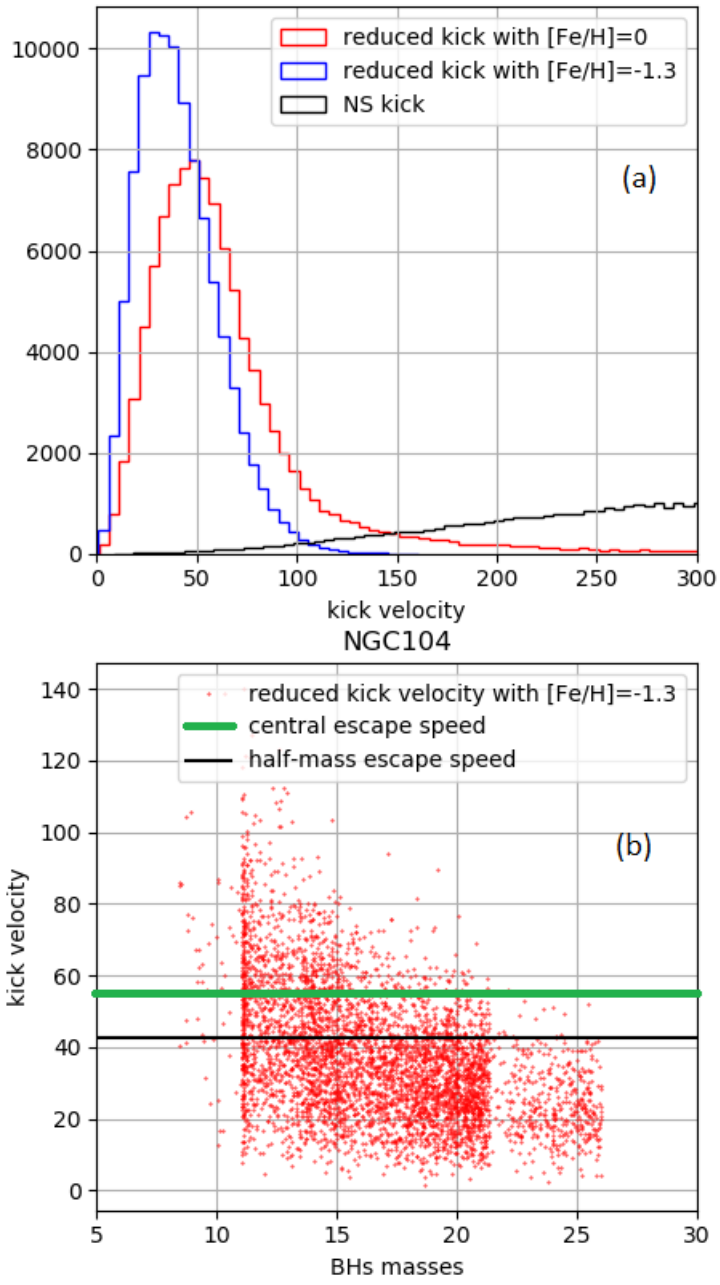

Figure 14: (a) The distribution of NS-kick(black), reduced kick with [Fe/H] equal 0(red) and -1.3(blue). Most of BHs can have kick velocity around 30 km/s or 50 km/s with [Fe/H]=0 or -1.3 respectively. (b) The BHs in NGC104 with reduced kick(with [Fe/H]=-1.3) velocity. Massive BHs are easier to be retained.

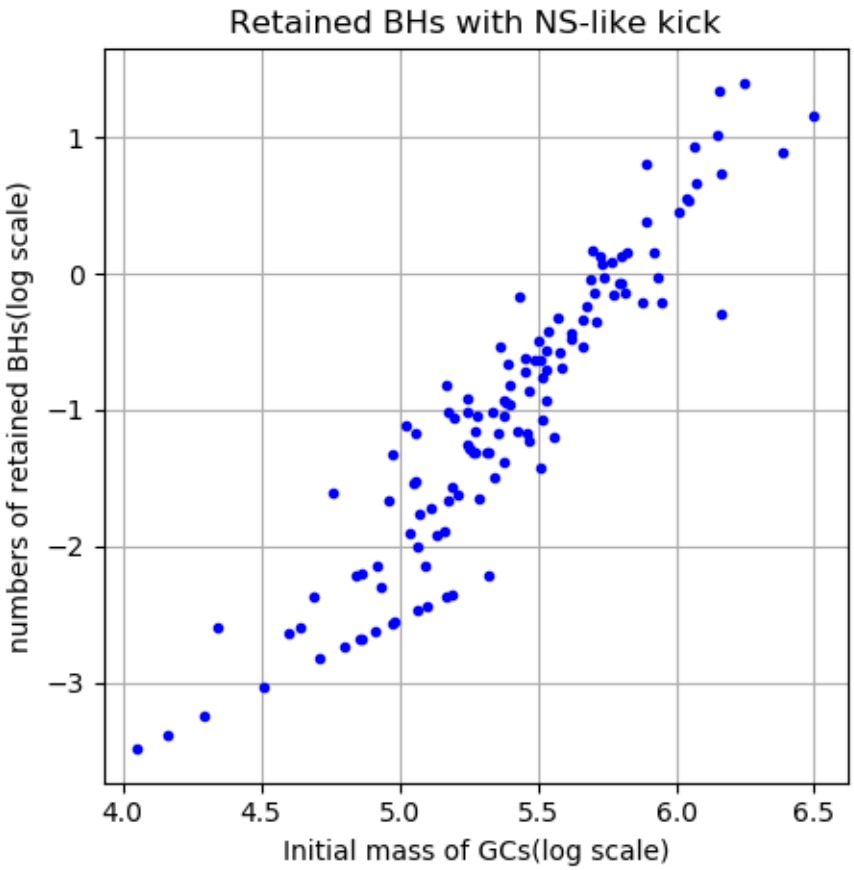

Figure 15: The scatter plot of retained BHs in GCs with NS-like kick and initial masses of GCs. More massive GCs could retain more BHs.

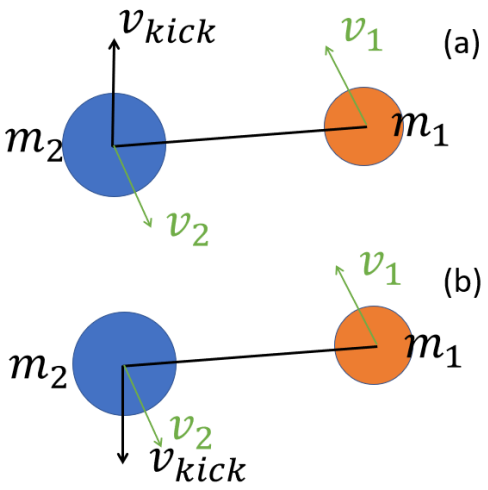

Figure 16: The two possible conditions after the supernova and their relationship to the direction of natal kick, the m_2 star is the black hole progenitor and m_1 star is the companion, v_1 and v_2 are the orbital velocities of the m_1 and m_2 stars before the supernova respectively. The v_{kick} is the kick velocity gave by natal kick. The condition (a) is more likely to be bound and (b) more likely to be unbound.

because the companions may slow them down. The Fig.16 shows the pre-supernova arrangement of massive star (m_2 star is the black hole progenitor) and its companion (m_1 star). There are two condition of the binary system after the supernova:(a) The two stars remain bound and have a $v_{com,new}$; (b) The massive star escape from the binary system and has a $v_{2,new}$. These two velocity($v_{com,new}$ and $v_{2,new}$) depend on the natal kick(v_{kick}) and mass-loss(ΔM). Whether the black hole remain in the globular cluster or not depends on the relationship between $v_{com,new}$(or $v_{2,new}$) and escape velocity.

In this section, I introduce distribution for binary properties, explain the energy fraction and calculate the retention of black holes in NGC104.

4.1 Binary properties

The distance a between two stars in one binary systems is related to their orbital period P. From the Kepler's Third law, we have

$$P^2 G(m_1 + m_2) = 4\pi^2 a^3 \tag{44}$$

Where $G = 39.478 AU^3 \cdot yr^{-2} \cdot M_{\odot}^{-1}$.

From the paper of Sana et al. (2012), the observed cumulative distributions for systems with known log of periods (34 in total) and mass-ratios (31 in total) are intrinsic distributions with power law exponents with $\pi = -0.55 \pm 0.22$ and $\kappa = -0.10 \pm 0.58$. The m_2 stars are O-type stars, I set the mass range of 20 to 70 solar mass. The distributions are from nearby open clusters because the massive stars (i.e. O-type stars) which can form black holes are today only found in open clusters. I assume here that the same distribution applies to globular clusters. The Fig.17 shows the distributions.

4.2 Bound or unbound

To investigate whether the binary system remains bound or not after the supernova, we can obtain the total energy (potential energy(U) plus kinetic energy(T)) after the supernovae. If this energy is smaller than zero, the two stars remain bound. In the simulation, I use the energy fraction which means the fraction of energy before and after supernova(E_{after}/E_{before}), a positive energy fraction means a bound binary system.

4.2.1 Energy fraction

Define V_{zmf} as the velocity of the Zero momentum frame (zmf), R_{zmf} as the location of Zero momentum frame. For the binary before supernovae, we have

$$V_{zmf} = \frac{dR_{zmf}}{dt} = \frac{d}{dt}(\frac{m_1 r_1 + m_2 r_2}{m_1 + m_2}) = \frac{m_1 v_1 + m_2 v_2}{m_1 + m_2} \tag{45}$$

Define u_1 and u_2 as the velocity relative to the zero momentum,

$$u_1 = v_1 - V_{zmf}, u_2 = v_2 - V_{zmf} \tag{46}$$

In Zero-momentum frame, p for momenta, we have the total momentum

$$p_1 + p_2 = m_1 u_1 + m_2 u_2 = 0 \tag{47}$$

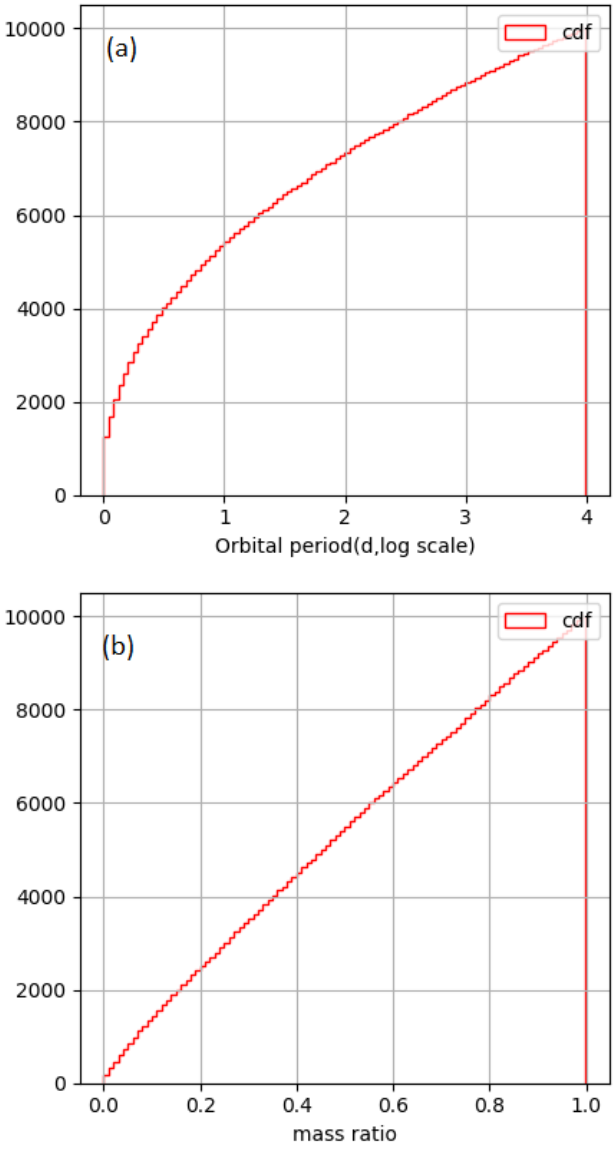

Figure 17: The cumulative distribution function of (a)log of periods in days and (b)mass-ratios taken from Sana et al. (2012). They are power law distribution with $\pi = -0.55$ and $\kappa = -0.10$.

So,

$$p_1 = m_1 u_1 = m_1(v_1 - V_{zmf}) = \frac{m_1 m_2}{m_1 + m_2}(v_1 - v_2) = -m_2 u_2 = -p_2 \tag{48}$$

where $\mu = \frac{m_1 m_2}{m_1 + m_2}$ is the reduced mass and $v_{rel} = v_1 - v_2$ is the relative velocity.

At last, the total kinetic energy before supernovae is

$$\begin{aligned} T &= \frac{1}{2} m_1 (\frac{m_2}{m_1 + m_2})^2 (v_1 - v_2)^2 + \frac{1}{2} m_2 (\frac{m_1}{m_1 + m_2})^2 (v_1 - v_2)^2 \\ &= \frac{1}{2} \frac{m_1 m_2^2 + m_2 m_1^2}{(m_1 + m_2)^2} (v_1 - v_2)^2 \\ &= \frac{1}{2} \frac{(m_1 + m_2) m_1 m_2}{(m_1 + m_2)^2} (v_1 - v_2)^2 \\ &= \frac{1}{2} \frac{m_1 m_2}{m_1 + m_2} (v_1 - v_2)^2 \\ &= \frac{1}{2} \mu v_{rel}^2 \end{aligned} \tag{49}$$

The potential energy,

$$U = \int_{\infty}^{a} F_G da = \int_{\infty}^{r} \frac{G m_1 m_2}{a^2} dr = -\frac{G m_1 m_2}{a} \tag{50}$$

In a circular orbit, the relative velocity

$$v_{rel} = v_1 - v_2 = \sqrt{\frac{G(m_1 + m_2)}{a}} \tag{51}$$

So, the relation between kinetic energy and potential energy,

$$T = \frac{1}{2} \mu v_{rel}^2 = -\frac{1}{2} U \tag{52}$$

The total energy before the supernova is

$$E_{before} = T + U = -\frac{1}{2} U + U = \frac{1}{2} U \tag{53}$$

For the binary system after supernova, we have

$$T_{new} = \frac{1}{2} \mu_{new} v_{rel,new}^2 \tag{54}$$

and

$$U_{new} = -\frac{Gm_1 m_{2,new}}{a} \tag{55}$$

Where T_{new} and U_{new} are total kinetic energy and total potential energy after supernovae.

Define the change of m_2 as δm and the kick velocity v_{kick} is a kick with random direction,

$$T_{new} = \frac{1}{2}\mu_{new} v_{rel}^2 = \frac{1}{2}\frac{m_1(m_2 - \delta m)}{m_1 + m_2 - \delta m}(v_1 - v_2 + v_{kick})^2 \tag{56}$$

and

$$U_{new} = -\frac{Gm_1(m_2 - \delta m)}{a} \tag{57}$$

$$U_{new} = U + \frac{Gm_1 \delta m}{a} \tag{58}$$

The total energy after supernova is

$$E_{after} = T_{new} + U_{new} \tag{59}$$

$$= \frac{1}{2}\frac{m_1(m_2 - \delta m)}{m_1 + m_2 - \delta m}(v_1 - v_2 + v_{kick})^2 + U + \frac{Gm_1 \delta m}{a} \tag{60}$$

For a bound binary system, total energy should smaller than zero.

At first, we can think about the zero mass-loss case and kick velocity of two special direction.

For the same direction of v_2, we have

$$E_{after} = T + U \tag{61}$$

$$= \frac{1}{2}\mu(v_{rel} + v_{kick})^2 - \mu v_{rel}^2 \tag{62}$$

$$= \frac{1}{2}\mu(v_{rel}^2 + 2v_{rel}v_{kick} + v_{kick}^2) - \mu v_{rel}^2 \tag{63}$$

$$= \frac{1}{2}\mu(-v_{rel}^2 + 2v_{rel}v_{kick} + v_{kick}^2) \tag{64}$$

Set energy equal zero for bound, the kick velocity is

$$v_{kick}^2 + 2v_{rel}v_{kick} - v_{rel}^2 = 0 \tag{65}$$

$$v_{kick} = \frac{-2v_{rel} + \sqrt{4v_{rel}^2 + 4v_{rel}^2}}{2} \tag{66}$$

$$v_{kick} = (\sqrt{2} - 1)v_{rel} \tag{67}$$

$$\tag{68}$$

Similar for the opposite direction,

$$E_{after} = T + U \tag{69}$$

$$= \frac{1}{2}\mu(v_{rel} - v_{kick})^2 - \mu v_{rel}^2 \tag{70}$$

$$= \frac{1}{2}\mu(-v_{rel}^2 - 2v_{rel}v_{kick} + v_{kick}^2) \tag{71}$$

$$v_{kick}^2 - 2v_{rel}v_{kick} - v_{rel}^2 = 0 \tag{72}$$

$$v_{kick} = \frac{2v_{rel} + \sqrt{4v_{rel}^2 + 4v_{rel}^2}}{2} \tag{73}$$

$$v_{kick} = (\sqrt{2} + 1)v_{rel} \tag{74}$$

$$\tag{75}$$

Fig.18 shows the relationship between energy fraction(E_{after}/E_{before}) and kick velocity. The kick velocity are generated from a Maxwellian distribution with $\sigma = 265km/s$. From this figure, we can see most of the binaries are unbound after the supernova. The kick from the opposite direction of v_2 increase the chance of remaining bound. There are no binary remaining bound with a kick in the same direction as v_2 in our simulation.

For the random mass-loss case, we get Fig.19. Compare to Fig.18, the results spread around the zero line. We can find the mass-loss fraction is less significant than kick velocity for the energy fraction.

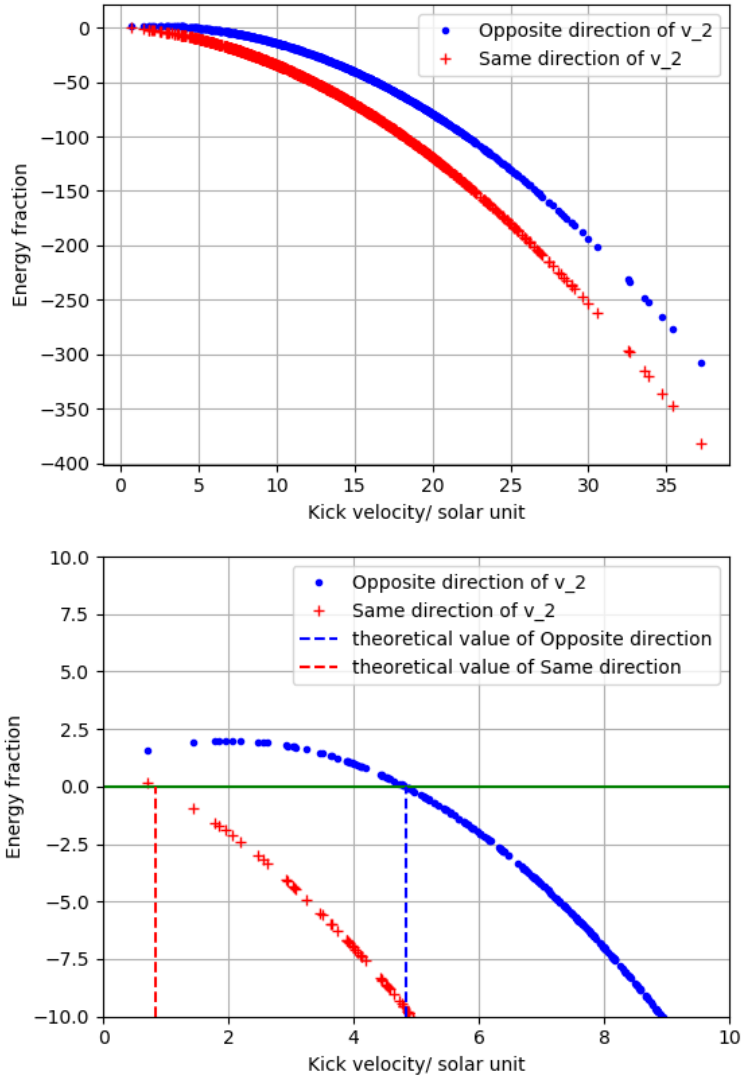

Figure 18: The Figure shows the kick velocity vs the energy fraction(E_{after}/E_{before}) in the zero mass loss case. The red cross for the natal kick is the same direction as the progenitor star's orbital velocity (v_2) and blue point for the opposite direction. The solar velocity unit means $\sqrt{\frac{GM_\odot}{AU}}$. The theoretical values of kick velocities in the second plot are $(\sqrt{2}-1)v_{rel}$ for v_2 direction and $(\sqrt{2}+1)v_{rel}$ for opposite direction. The relative velocity $v_{rel} = 2\sqrt{\frac{GM_\odot}{AU}}$. The value I choose for m_1, m_2 and a are $5M_\odot$, $15M_\odot$ and $5AU$. The second plot is the zoom of the area that the energy fraction from -10 to the 10 of the first plot. We can clearly see the theoretical values at the line of zero energy fraction in the second plot. This prove that the simulation we did is logical.

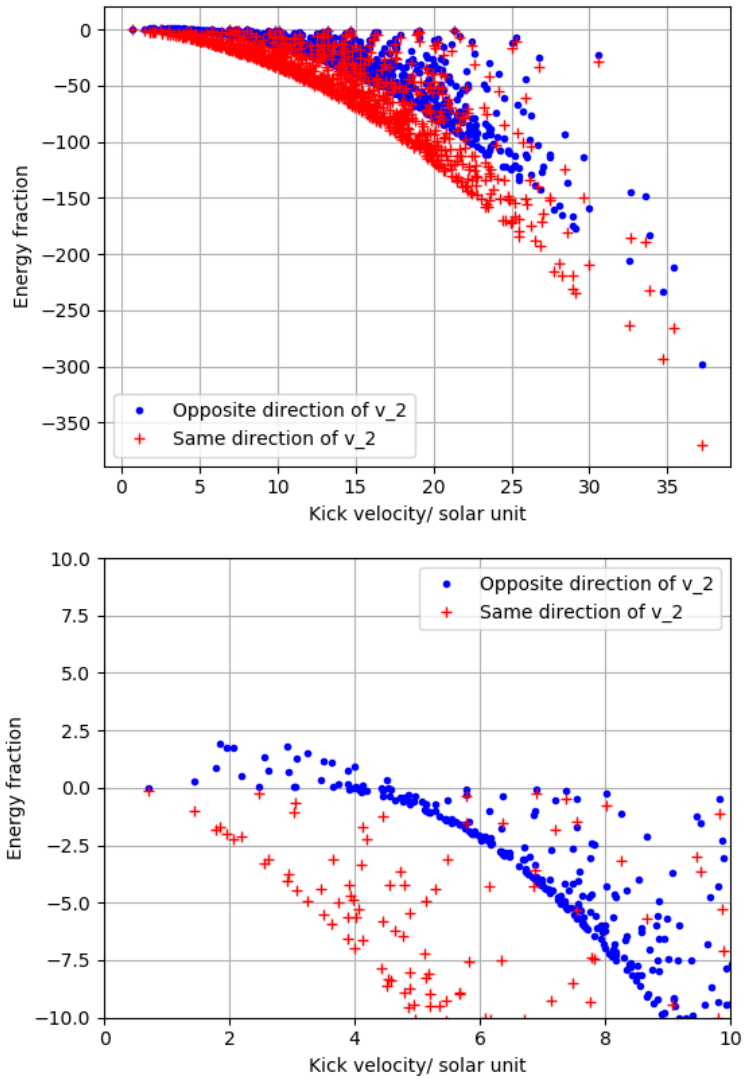

Figure 19: The Figure shows the kick velocity and energy fraction(E_{after}/E_{before}) with random mass lost (in $[0 : m_2]$) . The red cross for the natal kick is the same direction as the progenitor star's orbital velocity (v_2) and blue point for the opposite direction. The solar unit means $\sqrt{\frac{GM_\odot}{AU}}$.The value I choose for m_1, m_2 and a are $5M_\odot$, $15M_\odot$ and $5AU$. The second plot is the zoom of the area that the energy fraction from -10 to the 10 of the first plot. Compare to the Fig.18, under the same energy fraction, the value of kick velocity with mass lost is larger than the value of kick velocity with zero mass lost.

4.2.2 Bound binaries

For binary systems which remain bound, the retention of this system depend on the velocity of central mass v_{com}.

For a binary system after supernova, the momentum

$$\overrightarrow{p} = m_1\overrightarrow{v_1} + (m_2 - \delta m)(\overrightarrow{v_2} + \overrightarrow{v_{kick}}) \tag{76}$$

so the velocity of central mass

$$\overrightarrow{v_{com}} = \frac{\overrightarrow{p}}{m_1 + m_2 - \delta m} = \frac{m_1\overrightarrow{v_1} + (m_2 - \delta m)(\overrightarrow{v_2} + \overrightarrow{v_{kick}})}{m_1 + m_2 - \delta m} \tag{77}$$

4.2.3 Unbound binaries

For binary systems which are unbound, the m_2 star is also affected by the gravitational force from the m_1 star.

For the binary system after supernova,

$$E_{after} = T + U \tag{78}$$

$$= \frac{1}{2}\frac{m_1(m_2 - \delta m)}{m_1 + m_2 - \delta m}(v_1 - v_2 - v_{kick})^2 - \frac{Gm_1(m_2 - \delta m)}{a} \tag{79}$$

$$= \frac{1}{2}\mu_{new}v_{rel,new}^2 - \frac{Gm_1(m_2 - \delta m)}{a} \tag{80}$$

From the central of mass frame, we have

$$v_2 = \frac{m_1}{m_1 + m_2 - \delta m}v_{rel} \tag{81}$$

when the binary is unbound, v_2 effect by the gravitational force from m_1 star. At infinity, the gravitational potential energy equals zero

$$E_\infty = \frac{1}{2}\frac{m_1(m_2 - \delta m)}{m_1 + m_2 - \delta m}v_{\infty,rel}^2 = \frac{1}{2}\mu_{new}v_{rel,new}^2 - \frac{Gm_1(m_2 - \delta m)}{a} \tag{82}$$

$$v_{\infty,rel} = v_{rel,new}\sqrt{1 - \frac{2G(m_1 + m_2 - \delta m)}{av_{rel,new}^2}} \tag{83}$$

$$v_{\infty,2} = \frac{m_1}{m_1 + m_2 - \delta m} v_{rel,new} \sqrt{1 - \frac{2G(m_1 + m_2 - \delta m)}{a v_{rel,new}^2}} \tag{84}$$

Switch this to original frame, we have

$$v_{2,new} = v_{\infty,2} + v_{com} = \frac{m_1}{m_1 + m_2 - \delta m} v_{rel,new} \sqrt{1 - \frac{2G(m_1 + m_2 - \delta m)}{a v_{rel,new}^2}} + v_{com} \tag{85}$$

For each binary, the possibility of retention in cluster after the supernova depends on the final velocity of the m_2 star, v_{com} for bound binaries and $v_{2,new}$ for unbound binaries. This is only the situation that binaries will not interact before BHs form. The next section will explain how can we know they interact or not.

4.3 Interaction

In a binary system, the radius of two stars will increase during their evolution. If the radius exceed the Roche-lobe radius, two stars will interact. (Eggleton, 1983,Paczynski, 1971) The Roche-lobe is potential surface of a rotating reference frame surrounding both stars, the mass transfer will happen if one of two stars fills the Roche-lobe. For the binary population I generated in this project, the mass of the m_2 star is larger than the mass of the m_1 star. The m_2 star has a larger radius and evolve faster than the m_1 star. So, it is always the m_2 star fills the Roche-lobe first and cause the interaction.

The equation of Roche lobe radius (Eggleton, 1983) is

$$R_{RL}(t) = \frac{0.49 q(t)^{2/3}}{0.6 q(t)^{2/3} + ln(1 + q(t)^{1/3})} a_d(t) \tag{86}$$

where q is the mass-ratio for the star we calculate, a_d is the distance.

The equation of a_d is

$$a_d(t) = a_{d,0} \frac{m_{1,0} + m_{2,0}}{m_1(t) + m_2(t)} \tag{87}$$

where $a_{d,0}$ is the initial distance we calculated from the period.

So the Roche-lobe radius of m_2 star is

$$R_{RL}(t) = \frac{0.49\left(\frac{m_2(t)}{m_1(t)}\right)^{2/3}}{0.6\left(\frac{m_2(t)}{m_1(t)}\right)^{2/3} + ln(1+\left(\frac{m_2(t)}{m_1(t)}\right)^{1/3})} a_{d,0} \frac{m_{1,0}+m_{2,0}}{m_1(t)+m_2(t)} \tag{88}$$

and the Roche-lobe radius of m_1 star is

$$R_{RL}(t) = \frac{0.49\left(\frac{m_1(t)}{m_2(t)}\right)^{2/3}}{0.6\left(\frac{m_1(t)}{m_2(t)}\right)^{2/3} + ln(1+\left(\frac{m_1(t)}{m_2(t)}\right)^{1/3})} a_{d,0} \frac{m_{1,0}+m_{2,0}}{m_1(t)+m_2(t)} \tag{89}$$

The same as the IFMR of massive stars, the change of stellar mass through the time I use is from the stellar evolution routines of Hurley (2000). The data also include the radius and core mass of 1 to $100M_{\odot}$ star in solar metallicity([Fe/H]=0), [Fe/H]=-2 and [Fe/H]=-1.3.

Here I have two assumptions of interaction:(a) The binary merge: When two stars interact during main-sequence stage, they will merge and produce a new massive star with mass of m_1+m_2. (b) The common envelope evolution: If the m_2 already become a red giant before the interaction, the binary will have a large envelope during the mass transfer. This envelope will disappear during the common envelope evolution before the supernova of the m_2 star. As the m_2 star only has a core, we can assume that it will not get a natal kick after the supernova. This is because the natal kick comes from the asymmetric explosion which is affected by the surrounding material (envelope) of the star.

To determine the interaction of binaries, things we should consider are: (a) When the m_2 star fills the Roche-lobe: The parameters we need are Roche-lobe radius of m_2, radius of m_2 and the time. (b) At which stage the m_1 and m_2 stars interact: We should know the core mass of m_1 and m_2 when they interact. In the data of Hurley (2000), core mass equals zero means the main-sequence stage.

4.3.1 Binary merger

If the binaries merge, assuming the binaries do not lose mass during the merging, the mass of new star may be too large to produce a BH. For example, a binary system with $m_2 = 40M_\odot$ and $m_1 = 20M_\odot$ merge in the main-sequence stage, the mass of new star is about $60M_\odot$ which is still in BH mass range ($20-70M_\odot$). We can calculate the kick velocity as a single BH. But if we have a binary system with $m_2 = 60M_\odot$ and $m_1 = 30M_\odot$ merge in the main-sequence stage, the mass of new star is about $90M_\odot$ which is larger than $70M_\odot$. The new star will not become a BH, and we exclude it.

4.3.2 Common envelope evolution

For the common envelope evolution, there are two outcomes: (a) The m_1 star is in the main-sequence stage. After common envelope evolution, the m_1 star and the core of the m_2 star are left. (b) The m_1 star has already become a red giant. After common envelope evolution, the cores of two stars are left. These two conditions are the same for the BH progenitor. The natal kick of the BH is caused by the asymmetric explosion of the surrounding material of the star's core. We can assume that there are no natal kick because there are no or a little material surrounding the core when the supernova happens. In this case, all BHs formed in this kind of system will remain in the GCs.

4.4 Binary fraction

In the GC, most of the black hole progenitors are found in binary systems. But the fraction of those massive stars is still uncertain. In this project I set f_b as the fraction of binaries formed in binary system. For a GC, the numbers of retained BHs is

$$N_{BH,retained} = N_{BH,f}((1 - f_b)f_{BH,s} + f_b f_{BH,b}) \tag{90}$$

where $f_{BH,s}$ and $f_{BH,b}$ are the fractions of retained BH under the assumption of all BH progenitors are in single and binaries respectively.

Similar to the single BHs, I generate 10^5 random positions for binaries. For non-interacted binaries and merged binaries, I consider the NS-like kick and reduced kick. The binary fraction I choose is 3/4(0.75) because most of BHs progenitors are in binaries.

Fig.20, Fig.21 and Fig.22 show the numbers of retained BHs in GCs with NS-like kick and reduced kick under [Fe/H]=0, -1.3 and -2 respectively.

4.5 NGC104

For example, NGC104 is a cluster with $1.4573 \times 10^6 M_\odot$ and scale parameter $a = 4.14951pc$. The metallicity I used is [Fe/H]=-1.3. The number of formed BHs and the fraction of retained single BHs have already calculated in sec.3.2.4.

From the simulation, the $f_{BH,b}$ of NGC104 are 0.58073 (NS-like kick) and 0.71769 (reduced kick). The Fig.23 shows the number of retained BHs related to the fraction of binaries.

5 Conclusions and discussion

At first, assuming all BHs progenitors in GCs are single stars. For BH subsystem as a whole, even in massive GC like NGC104, NS-like kicks would lead to only a handful of BHs being retained in each cluster. Alternatively, reduced kicks gives hundreds to thousands of retained BHs in each cluster. Askar et al. (2018) showed that many GCs likely host subsystems of hundreds of BHs based on present-day kinematic properties of GCs. So, under the assumption that all BHs progenitors in GCs are single stars, the scenario of NS-like kicks should be excluded.

However, the possibility of retention will greatly increase if the BH progenitor has a bound companion. The Fig.23 shows that the numbers of retained BHs increase by the binary fraction in NGC104. From previous observation, we know that massive stars are usually found in binaries. Fig.20, Fig.21 and Fig.22 show that typical GCs retained $10^{2.5}$ BHs if $f_b = 3/4$ for both NS-like kicks and reduced kicks. From this, the scenario of NS-like kick cannot be ruled

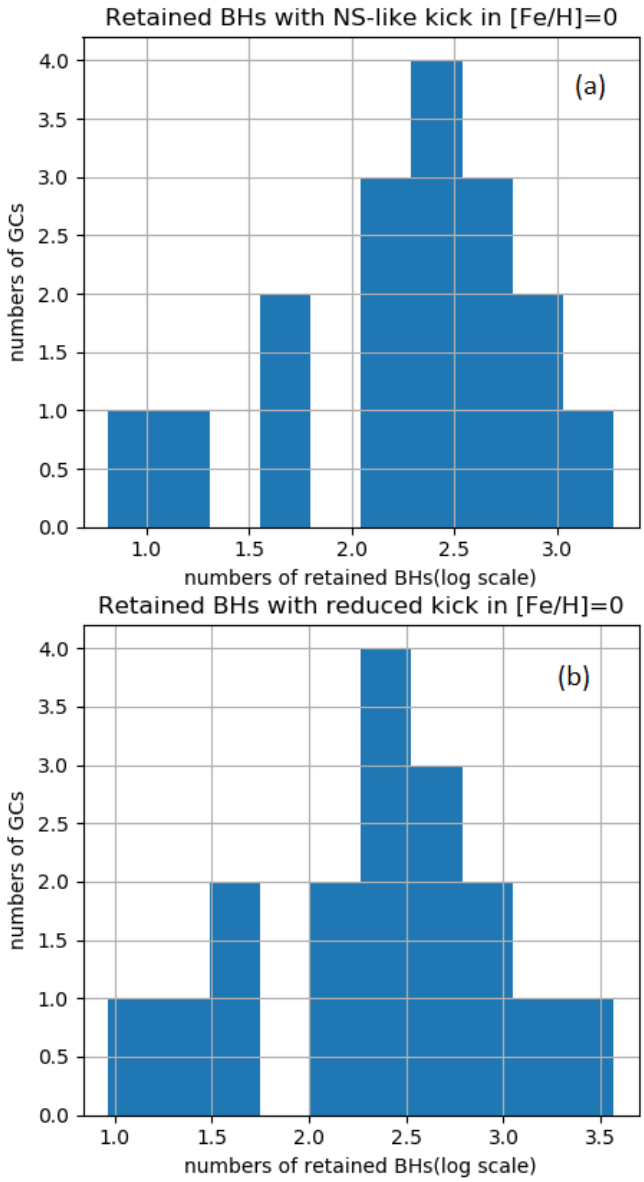

Figure 20: The histogram of retained BHs in GCs with (a) NS-like kick and (b) reduced kick under [Fe/H]=0. The binary fraction is 3/4(0.75) Most of GCs retain about $10^{2.5}$ BHs. The x-axis are the log scale of BHs numbers and y-axis are GCs numbers.

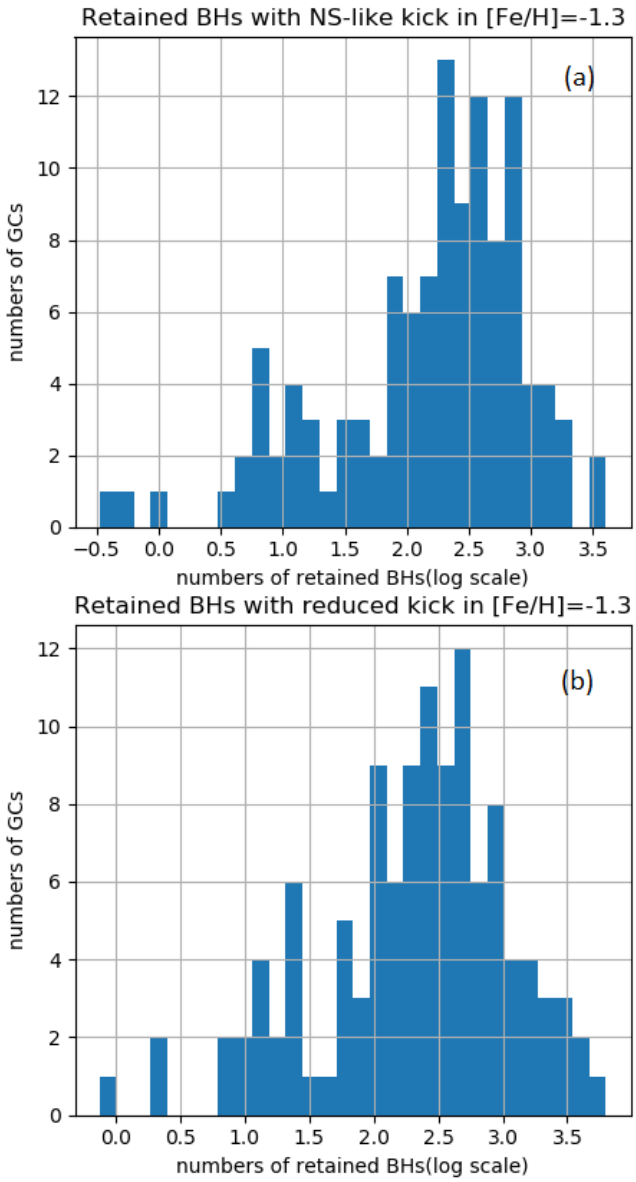

Figure 21: The histogram of retained BHs in GCs with (a) NS-like kick and (b) reduced kick under [Fe/H]=-1.3. The binary fraction is 3/4(0.75) Most of GCs retain about $10^{2.5}$ BHs. The x-axis are the log scale of BHs numbers and y-axis are GCs numbers.

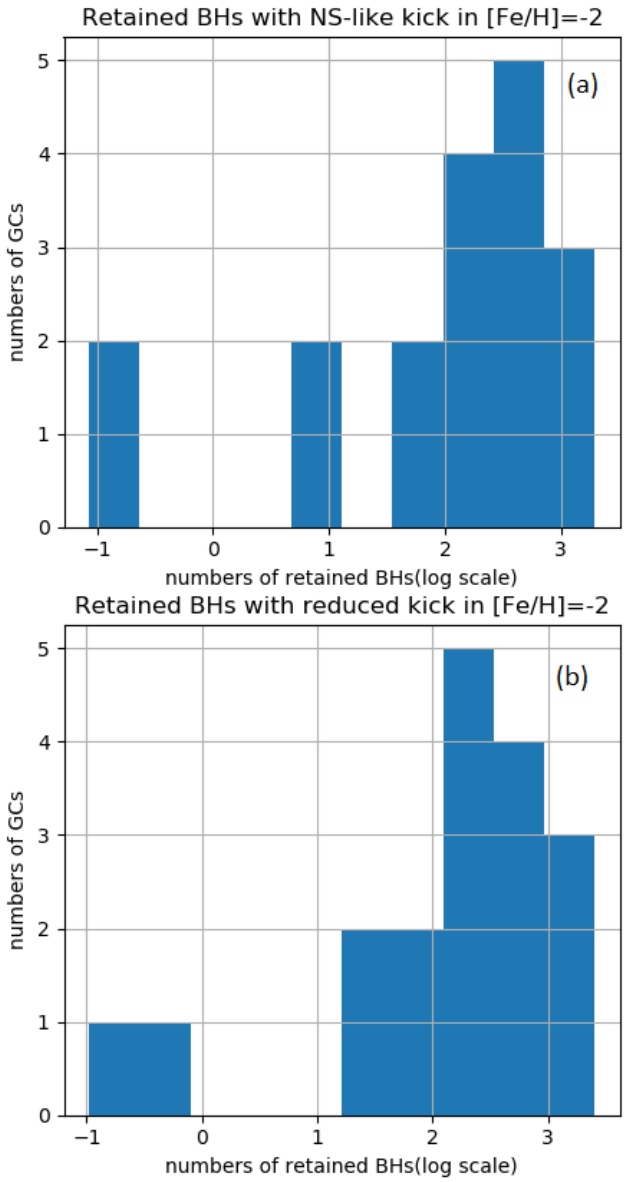

Figure 22: The histogram of retained BHs in GCs with (a) NS-like kick and (b) reduced kick under [Fe/H]=-2. The binary fraction is 3/4(0.75) Most of GCs retain about $10^{2.5}$ BHs. The x-axis are the log scale of BHs numbers and y-axis are GCs numbers.

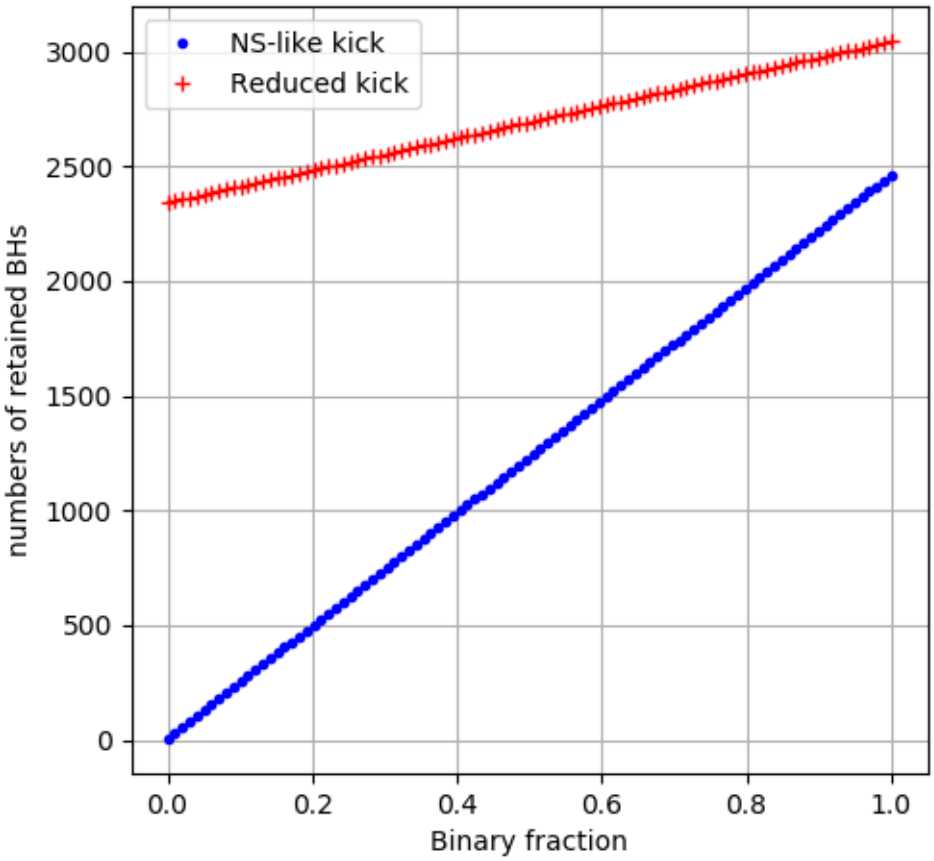

Figure 23: The figure of the number of retained BHs related to the fraction of binaries in NGC104. The blue points are NS-like kick and red cross are reduced kick.

out in a high binary fraction. This is not surprising in our simulation because the properties of binaries we use from Sana et al. (2012) gives closed binaries. If binaries are close, the potential energy of the companion is larger. So, more binaries remain bound or interact. Especially, the common envelope evolution during interaction of binaries removes the Hydrogen envelope and lead to a very low natal kick in our assumption.

In this project, I assume that the core-collapse of stripped massive stars gives low natal kick to the BHs. Actually, the magnitude of these kicks are still uncertain. If the kick is large, binaries will be less important for the retention of BHs.

Also, the binary fraction depends on metallicity and density of a given GC. GCs have lower metallicity or larger density may have larger binary fractions than others.

The properties of binaries from Sana et al. (2012) is for Open Clusters, it may not be reasonable in GCs. We still need to find some way of testing whether this applies in GCs. GCs have higher stellar density than OCs, so the fraction of closed binaries may be larger.

In conclusion, we have three parameters for the retention of BHs in GCs: (a) The NS-like kicks or the reduced kicks; (b) The binary fraction of cluster; (c) Binaries are closed or not. We can exclude the scenario of NS-like kicks in most situations except that the cluster has closed binaries.

References

Fabio Antonini, Roberto Capuzzo-Dolcetta, Alessandra Mastrobuono-Battisti, and David Merritt. Dissipationless Formation and Evolution of the Milky Way Nuclear Star Cluster. *apj*, 750(2):111, May 2012. doi: 10.1088/0004-637X/750/2/111.

Manuel Arca Sedda, Abbas Askar, and Mirek Giersz. MOCCA-Survey Database - I. Unravelling black hole subsystems in globular clusters. *mnras*, 479(4): 4652–4664, October 2018. doi: 10.1093/mnras/sty1859.

Z. Arzoumanian, D. F. Chernoff, and J. M. Cordes. The Velocity Distribution of Isolated Radio Pulsars. *apj*, 568(1):289–301, March 2002. doi: 10.1086/338805.

Abbas Askar, Manuel Arca Sedda, and Mirek Giersz. MOCCA-SURVEY Database I: Galactic globular clusters harbouring a black hole subsystem. *mnras*, 478(2):1844–1854, August 2018. doi: 10.1093/mnras/sty1186.

Abbas Askar, Melvyn B. Davies, and Ross P. Church. Formation of supermassive black holes in galactic nuclei - I. Delivering seed intermediate-mass black holes in massive stellar clusters. *mnras*, 502(2):2682–2700, April 2021.

Krzysztof Belczynski, Vassiliki Kalogera, and Tomasz Bulik. A Comprehensive Study of Binary Compact Objects as Gravitational Wave Sources: Evolutionary Channels, Rates, and Physical Properties. *apj*, 572(1):407–431, June 2002. doi: 10.1086/340304.

James Binney, Scott Tremaine, and Ken Freeman. Galactic Dynamics. *Physics Today*, 62(5):56, January 2009. doi: 10.1063/1.3141945.

Ross P. Church, Jay Strader, Melvyn B. Davies, and Alexey Bobrick. Formation Constraints Indicate a Black Hole Accretor in 47 Tuc X9. *apjl*, 851(1):L4, December 2017. doi: 10.3847/2041-8213/aa9aeb.

Ben Davies and Emma R. Beasor. 'On the red supergiant problem': a rebuttal, and a consensus on the upper mass cut-off for II-P progenitors. *mnras*, 496 (1):L142–L146, July 2020. doi: 10.1093/mnrasl/slaa102.

Steven De Gennaro, Ted von Hippel, D. E. Winget, S. O. Kepler, Atsuko Nitta, Detlev Koester, and Leandro Althaus. White Dwarf Luminosity and Mass Functions from Sloan Digital Sky Survey Spectra. *aj*, 135(1):1–9, January 2008. doi: 10.1088/0004-6256/135/1/1.

P. P. Eggleton. Aproximations to the radii of Roche lobes. *apj*, 268:368–369, May 1983. doi: 10.1086/160960.

Duncan A. Forbes and Terry Bridges. Accreted versus in situ Milky Way globular clusters. *mnras*, 404(3):1203–1214, May 2010. doi: 10.1111/j.1365-2966.2010.16373.x.

Gary S. Fraley. Supernovae Explosions Induced by Pair-Production Instability. *apss*, 2(1):96–114, August 1968. doi: 10.1007/BF00651498.

Brad M. S. Hansen and E. Sterl Phinney. The pulsar kick velocity distribution. *mnras*, 291(3):569–577, November 1997. doi: 10.1093/mnras/291.3.569.

William E. Harris. A Catalog of Parameters for Globular Clusters in the Milky Way. *AJ*, 112:1487, October 1996.

D. Helfand and J. Huang. *The origin and evolution of neutron stars: proceedings of the 125th Symposium of the International Astronomical Union, held in Nanjing, China, May 26-30, 1986.*, volume 125. January 1987.

G. Hobbs, D. R. Lorimer, A. G. Lyne, and M. Kramer. A statistical study of 233 pulsar proper motions. *mnras*, 360(3):974–992, July 2005.

J. R. Hurley. Nuclear and dynamical evolution of stellar systems. *The Observatory*, 120:426–427, December 2000.

John Kormendy and Douglas Richstone. Inward Bound—The Search For Supermassive Black Holes In Galactic Nuclei. *araa*, 33:581, January 1995. doi: 10.1146/annurev.aa.33.090195.003053.

Pavel Kroupa. On the variation of the initial mass function. *mnras*, 322(2): 231–246, April 2001. doi: 10.1046/j.1365-8711.2001.04022.x.

A. Kundu, T. J. Maccarone, and S. E. Zepf. Probing the Low Mass X-ray Binary-Globular Cluster Link in Early Type Galaxies. In *American Astronomical Society Meeting Abstracts*, volume 201 of *American Astronomical Society Meeting Abstracts*, page 108.06, December 2002.

R. B. Larson. Black hole remnants in globular clusters. *mnras*, 210:763–777, October 1984. doi: 10.1093/mnras/210.4.763.

A. D. Mackey and G. F. Gilmore. Comparing the properties of local globular cluster systems: implications for the formation of the Galactic halo. *mnras*, 355(2):504–534, December 2004. doi: 10.1111/j.1365-2966.2004.08343.x.

Ilya Mandel. Estimates of black hole natal kick velocities from observations of low-mass X-ray binaries. *mnras*, 456(1):578–581, February 2016. doi: 10.1093/mnras/stv2733.

NASA. Sun fact sheet, 2010. URL `https://nssdc.gsfc.nasa.gov/planetary/factsheet/sunfact.html`. Last accessed 17 July 2010.

B. Paczynski. Evolutionary Processes in Close Binary Systems. *araa*, 9:183, January 1971. doi: 10.1146/annurev.aa.09.090171.001151.

H. C. Plummer. On the problem of distribution in globular star clusters. *mnras*, 71:460–470, March 1911.

Florent Renaud, Oscar Agertz, and Mark Gieles. The origin of the Milky Way globular clusters. *mnras*, 465(3):3622–3636, March 2017. doi: 10.1093/mnras/stw2969.

Serena Repetto and Gijs Nelemans. Constraining the formation of black holes in short-period black hole low-mass X-ray binaries. *mnras*, 453(3):3341–3355, November 2015.

Serena Repetto, Melvyn B. Davies, and Steinn Sigurdsson. Investigating stellar-mass black hole kicks. *MNRAS*, 425(4):2799–2809, October 2012.

Serena Repetto, Andrei P. Igoshev, and Gijs Nelemans. The Galactic distribution of X-ray binaries and its implications for compact object formation and natal kicks. *mnras*, 467(1):298–310, May 2017.

H. Sana, S. E. de Mink, A. de Koter, N. Langer, C. J. Evans, M. Gieles, E. Gosset, R. G. Izzard, J. B. Le Bouquin, and F. R. N. Schneider. Binary Interaction Dominates the Evolution of Massive Stars. *Science*, 337(6093):444, July 2012. doi: 10.1126/science.1223344.

Agustin Sanchez-Lavega. An Introduction to Planetary Atmospheres, by A. Sanchez-Lavega. Scope: monograph. Level: undergraduate. *Contemporary Physics*, 52(5):487–487, September 2011. doi: 10.1080/00107514.2011.580060.

M. Seeds and D. Backman. *Astronomy: The Solar System and Beyond*. Cengage Learning, 2009. ISBN 9780495562030. URL `https://books.google.se/books?id=DajpkyXS-NUC`.

R. Teyssier. Cosmological hydrodynamics with adaptive mesh refinement. A new high resolution code called RAMSES. *aap*, 385:337–364, April 2002. doi: 10.1051/0004-6361:20011817.

B. Thorsbro, N. Ryde, R. M. Rich, M. Schultheis, F. Renaud, E. Spitoni, T. K. Fritz, A. Mastrobuono-Battisti, L. Origlia, F. Matteucci, and R. Schödel. Detailed Abundances in the Galactic Center: Evidence of a Metal-rich Alpha-enhanced Stellar Population. *apj*, 894(1):26, May 2020. doi: 10.3847/1538-4357/ab8226.

S. E. Woosley. Pulsational Pair-instability Supernovae. *apj*, 836(2):244, February 2017. doi: 10.3847/1538-4357/836/2/244.

Name	a,d_h(pc)	[Fe/H]	Mass(solar mass)	N_fBHs	f_BH,s_NS	f_BH,s_R	f_BH,b_NS	f_BH,b_R
NGC 104	4.15	-0.72	1.46E+06	4.24E+03	1.27E-03	5.52E-01	5.81E-01	7.18E-01
NGC 288	5.77	-1.32	1.25E+05	3.63E+02	2.00E-05	2.56E-02	4.87E-01	5.78E-01
NGC 362	2.05	-1.26	5.86E+05	1.71E+03	7.10E-04	4.76E-01	5.81E-01	7.11E-01
Whiting 1	1.93	-0.7	2.40E+03	6.98E+00	0.00E+00	4.70E-04	1.18E-01	4.13E-01
NGC 1261	3.22	-1.27	3.28E+05	9.54E+02	9.00E-05	1.87E-01	5.79E-01	5.95E-01
Pal 1	1.49	-0.65	2.53E+03	7.37E+00	0.00E+00	7.60E-04	1.86E-01	4.17E-01
AM 1	14.71	-1.7	1.94E+04	5.65E+01	0.00E+00	3.40E-04	1.52E-01	4.14E-01
Eridanus	12.06	-1.43	2.80E+04	8.16E+01	0.00E+00	1.05E-03	2.17E-01	4.36E-01
Pal 2	3.96	-1.42	3.83E+05	1.12E+03	1.80E-04	1.77E-01	5.80E-01	6.10E-01
NGC 1851	1.80	-1.18	5.34E+05	1.56E+03	8.70E-04	4.96E-01	5.81E-01	6.90E-01
NGC 1904	2.44	-1.6	3.46E+05	1.01E+03	3.70E-04	2.61E-01	5.32E-01	6.40E-01
NGC 2298	3.08	-1.92	8.31E+04	2.42E+02	3.00E-05	3.63E-02	4.61E-01	5.88E-01
NGC 2419	21.38	-2.15	1.46E+06	4.24E+03	1.20E-04	1.36E-01	6.16E-01	6.50E-01
Ko 2	2.12	-5	3.43E+02	9.99E-01	0.00E+00	1.00E-05	1.14E-01	1.40E-01
NGC 2808	2.23	-1.14	1.42E+06	4.13E+03	2.52E-03	7.51E-01	5.81E-01	7.04E-01
E 3	4.95	-0.83	1.11E+04	3.22E+01	0.00E+00	9.50E-04	2.29E-01	4.26E-01
Pal 3	17.49	-1.63	4.69E+04	1.37E+02	0.00E+00	1.40E-03	1.88E-01	4.32E-01
NGC 3201	4.42	-1.59	2.37E+05	6.91E+02	6.00E-05	8.81E-02	5.53E-01	6.05E-01
Pal 4	16.13	-1.41	6.30E+04	1.84E+02	1.00E-05	2.34E-03	2.97E-01	4.68E-01
Ko 1	3.65	-5	8.62E+02	2.51E+00	0.00E+00	3.00E-05	1.15E-01	2.52E-01
NGC 4147	2.69	-1.8	7.30E+04	2.13E+02	3.00E-05	3.54E-02	5.31E-01	5.81E-01
NGC 4372	6.60	-2.17	3.25E+05	9.46E+02	4.00E-05	9.24E-02	6.05E-01	6.13E-01
Rup 106	6.48	-1.68	8.62E+04	2.51E+02	0.00E+00	1.31E-02	1.66E-01	5.35E-01
NGC 4590	4.52	-2.23	2.21E+05	6.42E+02	5.00E-05	9.19E-02	5.49E-01	6.51E-01
NGC 4833	4.63	-1.85	4.61E+05	1.34E+03	2.20E-04	1.81E-01	5.79E-01	6.08E-01
NGC 5024	6.82	-2.1	7.58E+05	2.21E+03	2.80E-04	2.37E-01	6.26E-01	6.64E-01
NGC 5053	13.21	-2.27	1.26E+05	3.66E+02	1.00E-05	9.65E-03	3.52E-01	5.43E-01
NGC 5139	7.56	-1.53	3.16E+06	9.20E+03	1.54E-03	6.11E-01	5.81E-01	7.11E-01
NGC 5272	6.85	-1.5	8.86E+05	2.58E+03	2.40E-04	2.37E-01	5.76E-01	6.57E-01
NGC 5286	2.48	-1.69	7.79E+05	2.27E+03	1.05E-03	5.11E-01	5.81E-01	7.44E-01
AM 4	4.03	-1.3	1.32E+03	3.83E+00	0.00E+00	4.00E-05	1.17E-01	2.62E-01
NGC 5466	10.70	-1.98	1.54E+05	4.48E+02	1.00E-05	1.47E-02	2.65E-01	5.36E-01
NGC 5634	6.30	-1.88	2.96E+05	8.62E+02	7.00E-05	7.44E-02	4.84E-01	5.83E-01
NGC 5694	4.07	-1.98	3.37E+05	9.81E+02	1.20E-04	1.49E-01	5.75E-01	5.96E-01
IC 4499	9.35	-1.53	2.11E+05	6.13E+02	1.00E-05	2.72E-02	4.33E-01	5.72E-01
NGC 5824	4.20	-1.91	8.62E+05	2.51E+03	3.70E-04	3.69E-01	5.81E-01	6.50E-01
Pal 5	18.42	-1.41	2.91E+04	8.47E+01	0.00E+00	4.50E-04	1.78E-01	4.12E-01
NGC 5897	7.49	-1.9	1.94E+05	5.65E+02	4.00E-05	3.36E-02	5.32E-01	5.85E-01
NGC 5904	3.86	-1.29	8.31E+05	2.42E+03	5.90E-04	3.84E-01	5.76E-01	7.10E-01
NGC 5927	2.46	-0.49	3.31E+05	9.63E+02	1.80E-04	1.03E-01	4.76E-01	5.05E-01
NGC 5946	2.74	-1.29	1.85E+05	5.39E+02	9.00E-05	1.14E-01	5.35E-01	6.02E-01
BH 176	4.95	0	1.05E+04	3.05E+01	0.00E+00	2.20E-04	2.85E-01	4.06E-01
NGC 5986	2.96	-1.59	5.91E+05	1.72E+03	4.10E-04	3.61E-01	5.80E-01	6.59E-01
Lynga 7	2.79	-0.67	1.09E+05	3.16E+02	4.00E-05	5.85E-02	5.13E-01	5.89E-01
Pal 14	27.15	-1.62	2.07E+04	6.02E+01	0.00E+00	1.70E-04	1.37E-01	2.85E-01
NGC 6093	1.77	-1.75	4.87E+05	1.42E+03	6.50E-04	4.65E-01	5.80E-01	6.96E-01

NGC 6121	2.77	-1.16	1.87E+05	5.44E+02	1.30E-04	1.15E-01	5.73E-01	6.04E-01
NGC 6101	4.70	-1.98	1.48E+05	4.32E+02	1.00E-05	4.39E-02	5.57E-01	5.76E-01
NGC 6144	4.22	-1.76	1.37E+05	3.98E+02	3.00E-05	4.52E-02	5.60E-01	5.74E-01
NGC 6139	2.50	-1.65	5.49E+05	1.60E+03	5.80E-04	3.89E-01	5.79E-01	7.11E-01
Terzan 3	2.98	-0.74	2.11E+04	6.13E+01	0.00E+00	5.43E-03	3.74E-01	5.26E-01
NGC 6171	3.22	-1.02	1.75E+05	5.10E+02	1.10E-04	8.85E-02	5.52E-01	6.01E-01
1636-283	1.21	-1.5	1.01E+04	2.94E+01	0.00E+00	6.67E-03	4.07E-01	5.12E-01
NGC 6205	3.49	-1.53	6.54E+05	1.90E+03	3.80E-04	3.42E-01	5.80E-01	6.50E-01
NGC 6229	3.19	-1.47	4.16E+05	1.21E+03	2.70E-04	2.40E-01	5.80E-01	6.59E-01
NGC 6218	2.47	-1.37	2.09E+05	6.08E+02	8.00E-05	1.50E-01	5.80E-01	5.89E-01
FSR 1735	0.97	-5	9.45E+04	2.75E+02	1.70E-04	2.06E-01	6.22E-01	6.57E-01
NGC 6235	3.35	-1.28	8.16E+04	2.38E+02	1.00E-05	3.04E-02	5.39E-01	5.73E-01
NGC 6254	2.50	-1.56	2.44E+05	7.11E+02	1.60E-04	1.78E-01	4.82E-01	6.14E-01
NGC 6256	2.58	-1.02	1.80E+05	5.24E+02	1.00E-04	1.22E-01	5.77E-01	6.18E-01
Pal 15	14.43	-2.07	3.98E+04	1.16E+02	0.00E+00	1.66E-03	1.26E-01	4.79E-01
NGC 6266	1.82	-1.18	1.17E+06	3.40E+03	2.49E-03	7.53E-01	5.81E-01	7.87E-01
NGC 6273	3.38	-1.74	1.12E+06	3.25E+03	1.06E-03	5.29E-01	5.80E-01	7.43E-01
NGC 6284	2.94	-1.26	3.80E+05	1.11E+03	2.40E-04	2.41E-01	5.79E-01	6.20E-01
NGC 6287	2.02	-2.1	2.19E+05	6.36E+02	1.50E-04	2.28E-01	6.26E-01	6.78E-01
NGC 6293	2.46	-1.99	3.22E+05	9.37E+02	2.50E-04	2.40E-01	5.80E-01	6.35E-01
NGC 6304	2.44	-0.45	2.07E+05	6.02E+02	8.00E-05	5.59E-02	4.84E-01	5.14E-01
NGC 6316	1.97	-0.45	5.39E+05	1.57E+03	7.50E-04	2.42E-01	4.84E-01	5.82E-01
NGC 6341	2.46	-2.31	4.78E+05	1.39E+03	4.20E-04	4.00E-01	6.05E-01	7.28E-01
NGC 6325	1.43	-1.25	1.51E+05	4.40E+02	2.20E-04	1.94E-01	4.21E-01	6.13E-01
NGC 6333	2.21	-1.77	3.76E+05	1.10E+03	4.30E-04	3.13E-01	5.81E-01	6.31E-01
NGC 6342	1.80	-0.55	9.19E+04	2.68E+02	8.00E-05	8.15E-02	4.54E-01	5.97E-01
NGC 6356	3.56	-0.4	6.30E+05	1.84E+03	4.60E-04	1.44E-01	4.84E-01	5.01E-01
NGC 6355	2.36	-1.37	4.20E+05	1.22E+03	3.00E-04	3.25E-01	5.80E-01	6.55E-01
NGC 6352	3.34	-0.64	9.63E+04	2.80E+02	1.00E-05	3.85E-02	5.26E-01	5.74E-01
IC 1257	10.18	-1.7	7.17E+04	2.09E+02	1.00E-05	5.31E-03	3.95E-01	4.64E-01
Terzan 2	3.32	-0.69	5.59E+04	1.63E+02	0.00E+00	1.81E-02	2.93E-01	5.69E-01
NGC 6366	2.97	-0.59	4.92E+04	1.43E+02	3.00E-05	1.84E-02	3.80E-01	5.53E-01
Terzan 4	3.87	-1.41	1.54E+04	4.48E+01	0.00E+00	2.31E-03	2.71E-01	5.03E-01
HP 1	7.39	-1	9.54E+04	2.78E+02	0.00E+00	1.26E-02	4.51E-01	5.30E-01
NGC 6362	4.53	-0.99	1.50E+05	4.36E+02	5.00E-05	4.64E-02	3.61E-01	5.78E-01
NGC 6380	2.35	-0.75	2.49E+05	7.24E+02	2.10E-04	1.95E-01	5.80E-01	5.83E-01
Terzan 1	7.44	-1.03	1.44E+04	4.20E+01	1.00E-05	8.60E-04	1.84E-01	4.47E-01
Ton 2	3.10	-0.7	7.30E+04	2.13E+02	1.00E-05	2.85E-02	4.76E-01	5.63E-01
NGC 6388	1.50	-0.55	1.44E+06	4.20E+03	5.22E-03	8.61E-01	5.82E-01	8.10E-01
NGC 6402	3.52	-1.28	1.09E+06	3.16E+03	1.13E-03	5.03E-01	5.81E-01	6.93E-01
NGC 6401	5.89	-1.02	3.59E+05	1.05E+03	6.00E-05	1.04E-01	5.76E-01	5.93E-01
NGC 6397	1.94	-2.02	1.13E+05	3.28E+02	9.00E-05	1.12E-01	5.76E-01	6.61E-01
Pal 6	2.02	-0.91	1.29E+05	3.76E+02	5.00E-05	1.07E-01	5.77E-01	5.88E-01
NGC 6426	5.51	-2.15	1.16E+05	3.37E+02	1.00E-05	2.90E-02	4.82E-01	6.28E-01
Djorg 1	6.34	-1.51	1.54E+05	4.48E+02	6.00E-05	2.99E-02	5.31E-01	5.29E-01
Terzan 5	1.45	-0.23	2.31E+05	6.73E+02	4.30E-04	1.30E-01	4.84E-01	5.47E-01
NGC 6440	1.19	-0.36	7.86E+05	2.29E+03	2.81E-03	5.26E-01	4.85E-01	6.50E-01

NGC 6441	1.92	-0.46	1.77E+06	5.15E+03	4.88E-03	6.35E-01	4.86E-01	7.45E-01
Terzan 6	0.87	-0.56	2.70E+05	7.87E+02	8.60E-04	5.05E-01	5.76E-01	7.32E-01
NGC 6453	1.48	-1.5	1.92E+05	5.59E+02	1.60E-04	2.42E-01	5.79E-01	6.41E-01
NGC 6496	3.35	-0.46	1.89E+05	5.49E+02	9.00E-05	3.30E-02	4.13E-01	5.00E-01
Terzan 9	1.61	-1.05	7.58E+03	2.21E+01	0.00E+00	2.82E-03	2.42E-01	5.02E-01
Djorg 2	1.92	-0.65	1.57E+05	4.57E+02	1.90E-04	1.44E-01	5.79E-01	5.94E-01
NGC 6517	1.54	-1.23	4.96E+05	1.44E+03	1.01E-03	5.21E-01	5.80E-01	7.29E-01
Terzan 10	2.62	-1	8.62E+04	2.51E+02	2.00E-05	4.54E-02	4.94E-01	5.85E-01
NGC 6522	2.24	-1.34	2.85E+05	8.31E+02	2.30E-04	2.35E-01	5.80E-01	6.14E-01
NGC 6535	1.68	-1.79	1.97E+04	5.75E+01	1.00E-05	1.12E-02	3.29E-01	4.95E-01
NGC 6528	0.87	-0.11	1.06E+05	3.07E+02	2.50E-04	8.88E-02	4.84E-01	5.16E-01
NGC 6539	3.86	-0.63	5.15E+05	1.50E+03	3.00E-04	2.48E-01	5.80E-01	6.32E-01
NGC 6544	1.06	-1.4	1.48E+05	4.32E+02	3.50E-04	2.58E-01	5.80E-01	6.41E-01
NGC 6541	2.31	-1.81	6.36E+05	1.85E+03	7.20E-04	4.66E-01	5.81E-01	6.96E-01
2MS-GC01	1.73	-5	6.91E+04	2.01E+02	3.00E-05	7.12E-02	5.91E-01	6.46E-01
ESO-SC06	6.54	-1.8	2.21E+04	6.42E+01	0.00E+00	1.70E-03	1.29E-01	4.68E-01
NGC 6553	1.80	-0.18	3.19E+05	9.28E+02	3.50E-04	1.46E-01	4.84E-01	5.06E-01
2MS-GC02	0.78	-1.08	2.19E+04	6.36E+01	4.00E-05	3.75E-02	5.28E-01	5.11E-01
NGC 6558	4.63	-1.32	9.37E+04	2.73E+02	1.00E-05	2.31E-02	5.22E-01	5.82E-01
IC 1276	3.74	-0.75	1.16E+05	3.37E+02	3.00E-05	4.23E-02	4.87E-01	5.88E-01
Terzan 12	1.05	-0.5	1.13E+04	3.28E+01	1.00E-05	0.00E+00	0.00E+00	0.00E+00
NGC 6569	2.54	-0.76	5.10E+05	1.49E+03	4.90E-04	3.59E-01	5.80E-01	6.60E-01
BH 261	1.04	-1.3	1.18E+04	3.43E+01	0.00E+00	1.06E-02	4.16E-01	5.07E-01
NGC 6584	2.87	-1.5	2.96E+05	8.62E+02	1.60E-04	1.89E-01	5.78E-01	6.15E-01
NGC 6624	1.88	-0.44	2.46E+05	7.17E+02	3.00E-04	9.90E-02	4.84E-01	5.23E-01
NGC 6626	3.15	-1.32	4.57E+05	1.33E+03	3.50E-04	2.66E-01	5.77E-01	6.59E-01
NGC 6638	1.39	-0.95	1.75E+05	5.10E+02	1.90E-04	2.31E-01	5.80E-01	6.52E-01
NGC 6637	2.15	-0.64	2.83E+05	8.24E+02	2.90E-04	2.44E-01	5.52E-01	6.27E-01
NGC 6642	1.72	-1.26	1.15E+05	3.34E+02	9.00E-05	1.14E-01	5.35E-01	6.19E-01
NGC 6652	1.40	-0.81	1.15E+05	3.34E+02	2.00E-04	1.47E-01	5.79E-01	6.22E-01
NGC 6656	3.13	-1.7	6.25E+05	1.82E+03	4.70E-04	3.60E-01	5.45E-01	6.03E-01
Pal 8	2.16	-0.37	3.98E+04	1.16E+02	2.00E-05	6.12E-03	4.41E-01	4.88E-01
NGC 6681	1.86	-1.62	1.75E+05	5.10E+02	2.40E-04	1.70E-01	5.80E-01	6.25E-01
GLIMPSE01	0.79	-5	5.75E+04	1.67E+02	1.50E-04	1.45E-01	6.24E-01	6.66E-01
NGC 6712	2.67	-1.02	2.49E+05	7.24E+02	1.50E-04	1.68E-01	5.77E-01	6.13E-01
NGC 6715	6.32	-1.49	2.44E+06	7.11E+03	1.09E-03	5.84E-01	5.81E-01	6.15E-01
NGC 6717	1.40	-1.26	4.57E+04	1.33E+02	0.00E+00	4.64E-02	5.37E-01	5.83E-01
NGC 6723	3.87	-1.1	3.37E+05	9.81E+02	2.00E-04	1.57E-01	5.79E-01	6.16E-01
NGC 6749	2.53	-1.6	1.19E+05	3.47E+02	5.00E-05	7.42E-02	5.72E-01	5.89E-01
NGC 6752	2.22	-1.54	3.07E+05	8.95E+02	2.60E-04	2.53E-01	5.25E-01	6.30E-01
NGC 6760	2.73	-0.4	3.40E+05	9.90E+02	2.80E-04	9.48E-02	4.82E-01	5.42E-01
NGC 6779	3.01	-1.98	2.29E+05	6.66E+02	1.00E-04	1.35E-01	5.79E-01	6.20E-01
Terzan 7	5.11	-0.32	2.51E+04	7.31E+01	0.00E+00	9.60E-04	3.41E-01	3.34E-01
Pal 10	1.70	-0.1	5.15E+04	1.50E+02	1.00E-05	1.32E-02	4.58E-01	4.75E-01
Arp 2	14.73	-1.75	3.25E+04	9.46E+01	1.00E-05	1.10E-03	2.31E-01	4.53E-01
NGC 6809	4.45	-1.94	2.65E+05	7.72E+02	9.00E-05	9.92E-02	5.72E-01	5.91E-01
Terzan 8	7.27	-2.16	2.65E+04	7.72E+01	0.00E+00	2.35E-03	1.23E-01	5.09E-01

Pal 11	5.69	-0.4	1.46E+05	4.24E+02	3.00E-05	1.03E-02	4.15E-01	4.92E-01
NGC 6838	1.94	-0.78	4.36E+04	1.27E+02	2.00E-05	2.75E-02	4.05E-01	5.84E-01
NGC 6864	2.80	-1.29	6.66E+05	1.94E+03	7.30E-04	4.16E-01	5.74E-01	6.44E-01
NGC 6934	3.13	-1.47	2.37E+05	6.91E+02	1.30E-04	1.34E-01	5.78E-01	6.10E-01
NGC 6981	4.60	-1.42	1.63E+05	4.74E+02	5.00E-05	5.07E-02	4.99E-01	5.85E-01
NGC 7006	5.27	-1.52	2.91E+05	8.47E+02	8.00E-05	8.97E-02	5.45E-01	6.05E-01
NGC 7078	3.03	-2.37	1.18E+06	3.43E+03	1.35E-03	6.49E-01	6.27E-01	7.73E-01
NGC 7089	3.55	-1.65	1.02E+06	2.96E+03	9.60E-04	4.77E-01	5.81E-01	7.20E-01
NGC 7099	2.43	-2.27	2.37E+05	6.91E+02	1.70E-04	2.02E-01	6.26E-01	6.43E-01
Pal 12	9.51	-0.85	1.53E+04	4.44E+01	0.00E+00	6.10E-04	1.75E-01	3.77E-01
Pal 13	2.72	-1.88	7.94E+03	2.31E+01	0.00E+00	1.63E-03	2.40E-01	4.47E-01
NGC 7492	8.80	-1.78	5.24E+04	1.53E+02	0.00E+00	4.04E-03	2.59E-01	5.34E-01